Alma Mater Studiorum · Università di Bologna

Dipartimento di Fisica e Astronomia "Augusto Righi"
Corso di Laurea in Fisica

A geometric approach to the study of quantum systems: Berry's phase and topological quantum computation

Relatore:
Prof.ssa Elisa Ercolessi

Presentata da:
Alice Casagrande

Anno Accademico 2023/2024

Sommario

Il seguente elaborato si propone l'obiettivo di esplicitare ed analizzare le strutture geometriche che sottostanno ai processi fisici, in particolare quelli quantistici. Saranno definiti i concetti di geometria differenziale e topologia necessari, e l'analisi verrà condotta partendo dall'introduzione del concetto di fase di Berry, una fase acquisita dallo stato del sistema dopo aver compiuto un ciclo adiabatico. La sua scoperta, a opera del fisico M. V. Berry nei primi anni '80, è infatti storicamente riconosciuta come una svolta nel mondo della fisica, poiché ha sancito l'importanza della geometria nello studio di fenomeni fisici. Questo concetto verrà approfondito esplorando la sua natura nel contesto dei fibrati $U(1)$, per poi ampliarlo formulando l'esistenza di una fase di Berry "non-Abeliana". Altrettanta attenzione sarà data a quelli che sono gli aspetti geometrici e, soprattutto in questo caso, topologici, quando verrà presentato il concetto di computazione quantistica topologica. Questa metodologia di computazione potenzialmente rivoluzionaria mira a sfruttare le proprietà topologiche di particolari particelle, dette anyoni non-Abeliani, per ottenere tecnologie quantistiche immuni — o, quantomeno, particolarmente resistenti — alla decoerenza quantistica, una delle fonti di errore maggiormente complesse da gestire nel caso di computazione quantistica "convenzionale". Nel complesso, verrà dunque condotto uno studio di sistemi quantistici dal punto di vista matematico-geometrico, partendo da definizioni formali, passando per la descrizione di alcuni casi applicativi, fino all'impiego di questo approccio in vere e proprie applicazioni pratiche.

Abstract

This work intends to articulate and analyze the geometric structures underlying physical processes, particularly quantum ones. The necessary concepts of differential geometry and topology will be defined, and the analysis will begin with the introduction of the Berry's phase, a phase acquired by the state of the system when undergoing an adiabatic cycle. Its discovery, accomplished by physicist M. V. Berry in the early 1980s, is indeed recognized as a milestone in physics, since it affirmed the importance of geometry in the study of physical phenomena. This concept is further explored by examining its nature within the framework of $U(1)$ bundles, and later generalized to formulate the existence of "non-Abelian" Berry's phase. The same emphasis is given to the geometric and, in this case, also topological aspects, when addressing the concept of topological quantum computation. This potentially revolutionary approach to quantum computing seeks to exploit topological properties of a peculiar type of particles, known as non-Abelian anyons, in order to develop quantum technologies that are immune — or, at least, highly resistant — to quantum decoherence, one of the most challenging source of errors to manage in conventional quantum computation. Overall, a study of quantum systems from a mathematical-geometric point of view will be conducted, starting from formal definitions, passing through descriptions and applications to some applicative cases3., up to the use of this approach in real practical applications.

Contents

Introduction

This thesis aims to provide a geometric perspective on quantum systems by examining the mathematical structures underlying their behavior. Adopting such a point of view, not only enhances the visualization of physical problems, but also reveals unique and significant aspects intrinsic to these systems.

Moreover, this perspective can lead to a renewal of practical applications; specifically, the geometric and topological aspects of certain quantum systems underpin the emergence — particularly in the context of quantum computing — of topological quantum computation.

The foundational mathematical tools used throughout this work include manifolds, differential forms, holonomies, fiber bundles and group theory, together with key notions of topology. These concepts are introduced in Chapter 1 and in a subsection of Chapter 3, equipping the reader with the necessary background to approach the physical applications discussed in the remaining portions.

Chapter 2 focuses on the well-known concept of Berry's phase, i. e., the geometric phase acquired by the state of a quantum system which undergoes an adiabatic cycle. Its discovery in 1984 by the physicist M. V. Berry [1], marked the turning point, after which interest in geometric aspects of quantum mechanics was profoundly renewed. What is remarkable about Berry's phase is that, despite being a global phase, it has observable consequences in certain physical contexts. Furthermore, this phase depends exclusively on the geometry of the abstract parameter space, rather than the system's specific dynamics. More precisely, it will be demonstrated that Berry's phase, being deeply rooted in the geometric structure of the system's state space, is naturally described within the framework of $U(1)$ fiber bundles. In this context, related quantities such as Berry's connection and Berry's curvature are also defined, eventually leading to the interpretation of Berry's phase as a manifestation of holonomy [2].

In the same chapter, examples of Berry's phase emerging from physical systems are briefly analyzed. Our discussion will include a re-interpretation of the Aharonov-Bohm effect and a study of the degeneracy case. The latter is first examined through an analysis of a two-level system evolving *near* the degeneracy point in parameter space and is later generalized to introduce the concept of the non-Abelian Berry's phase [3].

Chapter 3, instead, intend to offer a general overview of the fundamental aspects of topological quantum computation, a way of performing quantum computation that exploits the topological properties of non-Abelian anyons to develop decoherence-free technologies — idea originally conceived in [4]. Anyons are *quasiparticles*, which may arise in physical systems constrained in two dimensions. They obey an exotic type of

statistics, distinct form those of bosons and fermions, referred to as *fractional* statistics. This statistical behavior is described by the so-called braid group, a non-Abelian group (in general), which characterize exchange of strands. Essentially, when two particles are exchanged in an anyonic system, the state evolves by acquiring either an arbitrary phase factor (in the case of Abelian anyons) or through a unitary matrix (for non-Abelian anyons). The presence of non-Abelian anyons in topological state of matter creates a degenerate subspace protected from local transformations. Adiabatic evolutions (obtained by *braiding*) of these anyons on such a space are described by the non-Abelian Berry's phase addressed in Chapter 2.

However, an introductory section about quantum computation — where concept such as qubits, quantum gates and decoherence are addressed — is clearly necessary before actually providing a characterization of topological computing. Parallelism between physics and their geometric interpretations are constantly highlighted, as they facilitate the comprehension of these concepts.

Finally, the last section is entirely dedicated to quantum topological computation [5]. A specific anyonic model, namely, that of Ising anyons, will be introduced. After mathematically describing how fusion and braiding of anyons occur, an actual example is presented where six anyons are used to create two qubits. It is demonstrated that two-qubit gates using anyons and braiding do coincide with "ordinary" quantum gates. Ultimately, it is noted that, in a real-world context, even topological computers would not be entirely decoherence-free.

In summary, this work aspires to analyze how geometric and topological methods provide powerful tools to describe and understand quantum systems. From the very central concept of Berry's phase, with its deep geometric roots, to the advanced framework of topological quantum computation, the intrinsic connection between mathematics and physical phenomena becomes evident. By examining both fundamental principles and practical applications, this thesis highlights the key insights that emerge when physics and geometry are brought together. In doing so, geometry and topology will be revealed not as mere abstract constructs but as indispensable frameworks for uncovering the hidden structures and mechanisms that govern quantum systems.

1 Differential geometry and fiber bundles

In this chapter, we introduce the essential mathematical and differential geometry concepts needed to understand the topics discussed in the following chapters.

1.1 Basic definitions

We shall start with basic concepts that will form the foundation of this chapter: we will explore definitions related to manifolds and vectors, and eventually address concepts such as tensors and differential forms.

1.1.1 Manifolds

A manifold $\mathcal{M}$ is a n-dimensional topological space that is locally homeomorphic[1] to the n-dimensional Euclidean space $\mathbb{R}^n$.
Thus, for every point $P \in \mathcal{M}$ there exists a map from an open neighbourhood $\mathcal{D}$:

$$\varphi : \mathcal{D} \to \mathbb{R}^n \tag{1.1}$$

that is continuous and 1-1 and which provides the *coordinates* x^μ to the point, so that $P = (x^1(P), x^2(P), \ldots, x^n(P))$.
The pair $(\mathcal{D}, \varphi)$ is called **chart**.
A set of charts which covers the whole manifold $\mathcal{M}$, that is $\mathcal{A} = \{\{(\mathcal{A}_i, f_i)\} : \mathcal{M} \subseteq \cup_i \mathcal{A}_i\}$, is called **atlas**.

The most common examples of manifolds are $\mathbb{R}^n$ and the S^2 sphere in $\mathbb{R}^3$; on the other hand, the surface of a cone is not a manifold. A more sophisticated example is represented by the phase space of a system consisting of N particles, which is a 6N-dimensional manifold [6].

A manifold $\mathcal{M}$ is said *homeomorphic* to $\mathcal{M}'$ if there exist an homeomorphism $\mathcal{F} : \mathcal{M} \to \mathcal{M}'$; in other words, $\mathcal{M}$ can be continuously transformed into $\mathcal{M}'$ and *vice versa*. For instance, a S^2 sphere is homeomorphic to an ellipsoid and the surface of a teacup is homeomorphic to the surface of a torus [7].
Furthermore, a manifold is *differentiable* if it admits a differentiable structure, meaning

[1] A map $f : A \to B$ from a space A onto the space B is said homeomorphism if it is continuous, 1-1 and such that its inverse φ^{-1} is also continuous.

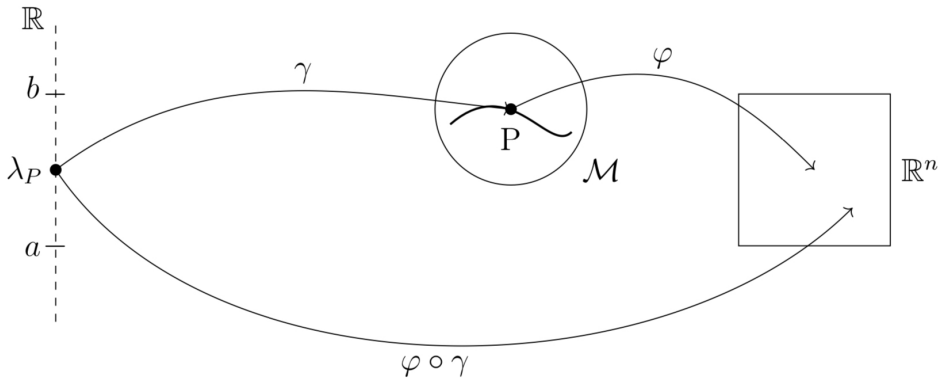

Fig. 1.1: Diagram showing the parameterized curve, with λ_P representing the parameter along the curve.

that smooth functions can be defined on it. More precisely, given any two different charts on $\mathcal{M}$, $(\mathcal{D}_1, \varphi_1)$ and $(\mathcal{D}_2, \varphi_2)$, such that $\mathcal{D}_1 \cap \mathcal{D}_2 \neq \varnothing$, the map:

$$\psi = \varphi_1 \circ \varphi_2^{-1} : \varphi_2(\mathcal{D}_1 \cap \mathcal{D}_2) \to \varphi_1(\mathcal{D}_1 \cap \mathcal{D}_2) \tag{1.2}$$

i.e., a *change of coordinates*, is k-times differentiable $\psi \in C^k$. If $\psi \in C^\infty$, the manifold is said *smooth*.
This differentiable structure allows the use of calculus on the manifold — which will be clearly independent from the coordinates chosen [7] for what we have just argued —, enabling formal definitions of notions such as derivatives, tangent spaces, and vector fields. Indeed, one of the most significant examples of a differentiable manifold is the vector space, that will be introduced in the next subsection.

According to their global[2] characteristics, manifolds are divided into classes: two manifolds $\mathcal{M}$, $\mathcal{M}''$ belong to the same class iff there exists a one-to-one and C^∞ map $\mathcal{G} : \mathcal{M} \to \mathcal{M}''$ and whose inverse $\mathcal{G}^{-1}$ is also C^∞ which is called *diffeomorphism* of $\mathcal{M}$ onto $\mathcal{M}''$. $\mathcal{M}$ and $\mathcal{M}''$ are said *diffeomophic* and the usual notation $\mathcal{M} \simeq \mathcal{M}''$. A diffeomorphism is always a homeomorphism, too.

Curves on a manifold.
Consider an open interval on the real line $I \subset \mathbb{R}$, $I = (a, b)$ and a manifold $\mathcal{M}$. A curve is a differentiable mapping[3] defined by [6]:

$$\gamma : I \subset \mathbb{R} \to \mathcal{M}. \tag{1.3}$$

[2]It follows from the definition itself that two manifolds of the same dimension are locally identical.
[3]By *differentiable mapping* we simply mean that the coordinates of the image point are functions belonging to C^k.

Now, a better definition can be formulated by taking into account the map $\varphi : \mathcal{M} \to \mathbb{R}^n$ in order to consider $\varphi \circ \gamma$:

$$\varphi \circ \gamma : I \subset \mathbb{R} \to \mathbb{R}^n \tag{1.4}$$

equivalent to:

$$x^i = x^i(\lambda), \quad \lambda \in (a, b), \quad i = 1, ..., n \tag{1.5}$$

which represents the parametrization of the curve in terms of the parameter λ.
The point P on the manifold is described by the image of the curve at parameter λ_P, with local coordinates $P = \{x^i(\lambda_P), i = 1, ..., n\}$ (see Fig.1.1).

1.1.2 Vector spaces

First of all, we shall define a *vector*, which, on a manifold, is usually defined as a vector tangent to a curve in $\mathcal{M}$. Let us see how.

Consider a curve in a n-dimensional manifold $\mathcal{M}$ passing through the point P, that is $x^i(\lambda)$ where λ is a parameter and $i = 1, ..., n$. A differentiable mapping $f : \mathcal{M} \to \mathbb{R}$ can be written as[4] $f(x^i) = f(x^1, ..., x^n)$. It will be defined for each point P of the curve $f(x^i(\lambda)) = g(\lambda)$ and thus, by differentiating with respect to the parameter, we get:

$$\frac{dg}{d\lambda} = \sum_i \frac{dx^i}{d\lambda} \left. \frac{\partial f}{\partial x^i} \right|_{\lambda=\lambda_P} \tag{1.6}$$

which has to held true *for any* function g (namely, for any set of coordinates expressed employing λ). Therefore we are allowed to write [6]:

$$\frac{d}{d\lambda} = \sum_i \frac{dx^i}{d\lambda} \frac{\partial}{\partial x^i} \,. \tag{1.7}$$

The latter is nothing but our definition of vector, which is, essentially, the definition of a tangent vector to the curve $x^i(\lambda)$: the terms dx^i are just infinitesimal displacements and dividing them by $d\lambda$ changes nothing apart from their "length". They are considered to be the *components* of the vector. Then, it is quite simple to understand that the other set of terms, $\partial/\partial x^i$, makes up the *basis* of a **vector space**.
Hence, we shall now consider a different curve $x^i(\mu)$ passing through the same point P in order to better analyze the definition 1.7. Once again, we are able to get to:

$$\frac{d}{d\mu} = \sum_i \frac{dx^i}{d\mu} \frac{\partial}{\partial x^i} \,. \tag{1.8}$$

[4]There actually actually is an abuse of notation, as f really is $f \circ \varphi^{-1}$.

Given a, b two scalars, we can linearly combine the two vectors [6]:

$$a\frac{d}{d\lambda} + b\frac{d}{d\mu} = \sum_i \left(a\frac{dx^i}{d\lambda} + b\frac{dx^i}{d\mu} \right) \frac{\partial}{\partial x^i} = \frac{d}{d\nu} \tag{1.9}$$

which is exactly the expression of another tangent vector $d/d\nu$ whose components are $a(dx^i/d\lambda) + b(dx^i/d\mu)$.
It is now straightforward to associate all the vectors tangent at the same point P with a *vector space* whose basis e_i consists of vectors of the form $\partial/\partial x^i$. In particular, the vector space is the **tangent vector space**: for each point $P \in \mathcal{M}$ it is possible to attach a copy of $\mathbb{R}^n$, called the tangent vector space [8] it is denoted by $T_P\mathcal{M}$ and its dimension equals the manifold's dimension.

We can conclude by pointing out that, in this way, the one-to-one correspondence between tangent vectors and derivatives along the curve becomes clear.

Remark. This point of view is convenient as it does not rely on the concept of coordinates and, moreover, it is naturally connected to the concept of motion along the curve (derivative) [6].

We shall now fix the notation[5]. $\mathbf{V}$ denotes a vector, while the numbers V^i represent the components:

$$\mathbf{V} = \sum_i V^i \frac{\partial}{\partial x^i} \tag{1.10}$$

Consider a point P on the manifold such that $P \in \mathcal{D}_1 \cap \mathcal{D}_2$ and let $\varphi_1(P) = \{x^1(P),$ $..., x^n(P)\}$ and $\varphi_2(P) = \{y^1(P), ..., y^n(P)\}$ be the maps that provides two different sets of coordinates for P. Then, a vector $\mathbf{V}$ can be expressed through two equivalent expressions [7]:

$$\mathbf{V} = \sum_i V^i \frac{\partial}{\partial x^i} = \sum_j V'^j \frac{\partial}{\partial y^j} \tag{1.11}$$

where V^i, V'^j stand for two different sets of components of the vector. From (1.11), two elements from the two different sets have the following relation:

$$V'^j = V^i \frac{\partial y^j}{\partial x^i}\,. \tag{1.12}$$

It is possible to find a basis for each $T_P\mathcal{M}$, resulting in a basis for the tangent space at each point on the manifold, which we refer to as the basis of a **vector field** [6]. This allows us to fix a tangent vector for each point on the manifold.

[5] In many cases, the sum will be implicit, using *Einstein's notation.*

Indeed, a vector field on a n-dimensional manifold $\mathcal{M}$ is a C^∞ map $\bar{V} : \mathcal{M} \to \mathbb{R}^n$ which assigns a vector $\mathbf{V}_P$ to each point $P \in \mathcal{M}$ [7].
Note that, from now on, we shall consider the concepts of vector and vector field practically interchangeable, expressing also an arbitrary vector field with the notation used in (1.8) or (1.10).

Let us introduce an useful function, called *pushforward* of smooth functions.
Consider $\Phi : \mathcal{M} \to \mathcal{N}$ a smooth map between two smooth manifolds; the pushforward (or differential) of Φ at $P \in \mathcal{M}$ is a linear map defined as:

$$\Phi_{*P} : T_p\mathcal{M} \to T_{f(P)}\mathcal{N},$$

that acts on a tangent vector $\mathbf{V} \in T_P\mathcal{M}$ by:

$$(\Phi_{*P}\mathbf{V}_P)(g) = \mathbf{V}(g \circ \Phi),$$

for any smooth function g near $\Phi(P)$.

Before moving on, let's define one last concept.
Given two vector fields $\bar{V} = d/d\lambda = V^i\partial/\partial x^i$ and $\bar{W} = d/d\mu = W^j\partial/\partial x^j$, it is useful to introduce an operator, the **commutator**, also known as *Lie brackets*, which is defined as [6]:

$$\left[\bar{V}, \bar{W}\right] = \left[\frac{d}{d\lambda}, \frac{d}{d\mu}\right] = \left(V^i\frac{\partial W^j}{\partial x^i} - W^i\frac{\partial V^j}{\partial xi}\right)\frac{\partial}{\partial x^j}\,. \tag{1.13}$$

The significant result is that we obtain a new vector field whose components are defined by the terms in the parentheses.

1.1.3 Tensors and differential forms

One-forms
Because of the vectorial nature of $T_P\mathcal{M}$, there exists also the correspondent, so-called, **dual** tangent **space** $T_P^*\mathcal{M}$, made up of the linear functions $\tilde{\omega}$ such that:

$$\tilde{\omega} : T_P\mathcal{M} \to \mathbb{R}\,. \tag{1.14}$$

These are called dual vectors, cotangent vectors or one-forms.
Now, given $\mathbf{V} \in T_P\mathcal{M}$, an important relation holds between $\mathbf{V}$ and $\tilde{\omega}$ [6]:

$$\tilde{\omega}(\mathbf{V}) \equiv \mathbf{V}(\tilde{\omega}) \equiv \langle\tilde{\omega}, \mathbf{V}\rangle \in \mathbb{R} \tag{1.15}$$

which shows the fact that we can see one-forms and vectors as linear functions of each other that provide the same real number.

The last term of 1.15 points out this "symmetry" connecting the two mathematical objects; the operator:

$$\langle \cdot, \cdot \rangle : T_P^*\mathcal{M} \times T_P\mathcal{M} \to \mathbb{R} \tag{1.16}$$

is called *inner product*.
It can be explicitly written as [7]:

$$\langle \tilde{\omega}, \mathbf{V} \rangle = \omega_\mu V^\nu \left\langle dx^\mu, \frac{\partial}{\partial x^\nu} \right\rangle = \omega_\mu V^\nu \delta^\mu_\nu = \omega_\mu V^\mu \tag{1.17}$$

A one-form can be expressed in component form as:

$$\tilde{\omega} = \omega_\mu dx^\mu. \tag{1.18}$$

where dx^μ is the dual form of the basis vector ∂/∂_ν, such that: $\langle x^\mu, \partial/\partial_\nu \rangle = \delta_{\mu\nu}$, with $\delta_{\mu\nu}$ Kronecker delta function.

An example of one-form is the differential df of a scalar function $f : \mathcal{M} \to \mathbb{R}$ [7].

Tensors
A (q, r) tensor is a multilinear object such that, given q one-forms $\tilde{\omega} \in T_P^*\mathcal{M}$ and r vectors $\mathbf{V} \in T_P\mathcal{M}$:

$$\mathbb{T} : \otimes^q T_P^*\mathcal{M} \otimes^r T_P\mathcal{M} \to \mathbb{R} \tag{1.19}$$

where $\otimes$ is the *tensor product*[6].
Trivially, a (0, 0) tensor is a scalar. A (1, 0) tensor is a vector, as it takes as argument a one-form, while a (0, 1) tensor is a one-form because it takes as argument a vector.

Differential forms
A r-form is a totally antisymmetric[7] tensor of type (0, r).

We shall now focus on one operation that transfer a one form from a manifold to another: the *pullback* of forms.
Consider $\mathcal{M}$ and $\mathcal{N}$ two differentiable manifolds and $\Phi : \mathcal{M} \to \mathcal{N}$ a smooth map between them. If $\tilde{\omega}$ is a k-form on $\mathcal{N}$, then the pullback of $\tilde{\omega}$ by Φ, denoted by $\Phi^*\tilde{\omega}$, is a k-form on $\mathcal{M}$. Clearly, k must be less- or equal, at the utmost,- than the dimensions of the manifolds, which are not necessarily the same.
Let us see how a pullback $(\Phi^*\tilde{\omega})$ acts:

$$(\Phi^*\tilde{\omega})(\mathbf{V}_1, ..., \mathbf{V}_k) = \tilde{\omega}(d\Phi(\mathbf{v}_1), ..., d\Phi(\mathbf{V}_k)\,. \tag{1.20}$$

[6]The tensor product of two vector spaces is defined as the vector space spanned by all possible products of the basis elements from each of the two original spaces.

[7]A totally antisymmetric tensor is defined as a tensor which acquires a negative sign every time an index is interchanged: $T^{i_1,...,i_k,...,i_j,...,i_n} = -T^{i_1,...,i_j,...,i_k,...,i_n}$.

Here, $\mathbf{V}_1, ..., \mathbf{V}_k$ are k vectors on $\mathcal{M}$ (or, more precisely, on $T_P\mathcal{M}$, P is the point on which the pullback acts) and $d\Phi(\mathbf{V}_1), ..., d\Phi(\mathbf{V}_k)$ are the *pushforwards of the vectors* by Φ, i. e., the linear mapping $d\Phi : T_P\mathcal{M} \to T_{\Phi(P)}\mathcal{N}$.

1.2 Exterior calculus for differential forms

This section will address the basics of calculus with differential forms, a powerful tool that generalizes the multivariable calculus of vectors.
We define the wedge product, introduce the exterior derivative, discuss integration with forms, and briefly touch on the generalized Stokes's theorem.

1.2.1 Wedge product

It is possible to define an associative and bilinear operation $\wedge$, called **wedge product**, that combines two differential forms into a higher-degree form. Specifically, given $\tilde{p}$ a p-form and $\tilde{q}$ a q-form, their wedge product $\tilde{p} \wedge \tilde{q}$ will be a $(p+q)$-form and it holds [6]:

$$\tilde{p} \wedge \tilde{q} = (-1)^{pq} \tilde{q} \wedge \tilde{p}\,. \tag{1.21}$$

For example, we can obtain a two-form from two one-forms:

$$\tilde{p} \wedge \tilde{q} = \tilde{p} \otimes \tilde{q} - \tilde{q} \otimes \tilde{p} \tag{1.22}$$

and a three-form from three one-forms:

$$\begin{aligned} \tilde{p} \wedge (\tilde{q} \wedge \tilde{r}) &= (\tilde{p} \wedge \tilde{q}) \wedge \tilde{r} = \tilde{p} \wedge \tilde{q} \wedge \tilde{r} \\ &= \tilde{p} \otimes \tilde{q} \otimes \tilde{r} + \tilde{r} \otimes \tilde{p} \otimes \tilde{q} + \tilde{q} \otimes \tilde{r} \otimes \tilde{p} \\ &\quad - \tilde{p} \otimes \tilde{r} \otimes \tilde{q} - \tilde{r} \otimes \tilde{q} \otimes \tilde{p} - \tilde{q} \otimes \tilde{p} \otimes \tilde{r} \end{aligned} \tag{1.23}$$

and so on.
This operator is very useful as it helps to simplify calculus on manifolds.

In addition, it allows us to write a r-form in the following form:

$$\tilde{\omega} = \sum_{1 \le i_1 < i_2 < ... < i_r \le n} \omega_{i_1 i_2 ... i_r} dx^{i_1} \wedge dx^{i_2} \wedge ... \wedge dx^{i_r} \tag{1.24}$$

where n is the dimension of the manifold on which the differential form is defined and $dx^1, ..., dx^n$ is a local basis for $T_P^*\mathcal{M}$ made up of one-forms, while $\omega_{i_1 i_2 ... i_r}$ are smooth scalar functions which embody the r-form coordinates.

1.2.2 Exterior derivative

The **exterior derivative** of a r-form is a linear operator d which maps a r-form in a $(r+1)$ form:

$$d : \Omega^r(\mathcal{M}) \to \Omega^{r+1}(\mathcal{M}) \tag{1.25}$$

where Ω^k is the k-forms space on the manifold $\mathcal{M}$.
An exterior derivative $d\tilde{\omega}$ of an arbitrary r-form $\tilde{\omega}$ on $\mathcal{M}$ must satisfy [6]:

$$d(d\tilde{\omega}) = 0; \tag{1.26}$$

$$d(\tilde{\omega} + \tilde{\eta}) = d\tilde{\omega} + d\tilde{\eta} \quad \forall \tilde{\omega}, \tilde{\eta} \in \Omega^r(\mathcal{M}); \tag{1.27}$$

$$d(\tilde{\omega} \wedge \tilde{\eta}) = d\tilde{\omega} \wedge \tilde{\eta} + (-1)^r \tilde{\omega} \wedge d\tilde{\eta} \quad \forall \tilde{\omega} \in \Omega^r(\mathcal{M}), \tilde{\eta} \in \Omega^l(\mathcal{M})\,. \tag{1.28}$$

Just as a rule which defines a vector can be associated to each point on the manifold, the same result can be achieved with differential forms; a **field of one-forms** $\bar{\tilde{\omega}}$ is a rule which associates a differential form $\tilde{\omega} \in T_P^*\mathcal{M}$ to each point of the manifold $P \in \mathcal{M}$. We can thus naturally define the following function $\bar{\tilde{\omega}}(\bar{V})$ relating vectors fields and fields of one-forms. Note the similarity with (1.15).

The standard differential operator d, which we cited in 1.1.3, is itself an example of exterior derivative [6]: a scalar function f can be seen as a zero-form and df is indeed a one-form. This means that, for f scalar function, the field of one-forms df is the analogous of the gradient:

$$df\left(\frac{d}{d\lambda}\right) = \frac{df}{d\lambda}\,. \tag{1.29}$$

In a similar way, we can say that $d\tilde{\omega}$ is the analogous of the curl when $\tilde{\omega}$ is a one-form, while it represents the analogous of the divergence when $\tilde{\omega}$ is a two-form.

1.2.3 Integration with differential forms

It is fundamental to firstly understand the concept of orientation[8] for a manifold.

A manifold $\mathcal{M}$ is said to be **orientable** if, given two arbitrary coordinates charts, such as $(\mathcal{D}, \varphi)$ with coordinates x^μ and $(\mathcal{D}', \varphi')$ with coordinates y^α, the determinant of the Jacobian matrix for the change of coordinates satisfies: $J = det(\partial x^\mu / \partial y^\alpha) > 0$.

The fact that the determinant is greater than zero implies that the two charts have the same orientation. If it were less than zero for even a single pair of charts, it would be impossible to find a consistent orientation for the entire manifold, as the two charts

[8] Orientation allows us to define a "positive" direction for an n-form, where n is the dimension of the manifold.

would have opposite orientations [7].
The Euclidean space $\mathbb{R}^n$ and the S^2 sphere are examples of orientable manifolds; a classical example of non-orientable manifold is instead the Möbius strip.

The existence of a globally non-vanishing n-form $\tilde{\omega}$ on an orientable n-dimensional manifold is guaranteed by the manifold's orientability [9]. The global defined n-form $\tilde{\omega}$ is called *volume form* and it essentially plays the role of "measure" when integrating a scalar function f over the manifold [7]:

$$\int_{\mathcal{M}} f\tilde{\omega} \equiv \int_{\varphi(\mathcal{D}_i)} f(\varphi^{-1}(x))\omega(\varphi^{-1}(x))dx^1 \wedge ... \wedge dx^n \,. \tag{1.30}$$

Here, $(\mathcal{D}_i, \varphi_i)$ represent different charts in which the n-form can be expressed through the $\omega(\varphi^{-1}(x))$ coefficients as in (1.24). An important feature of (1.30) is that the choice of the atlas, i.e., the choice of coordinates, does not affect the final form of the expression [7].

A crucial result for the theory of exterior calculus is the *generalized Stokes's theorem.*

Theorem. *Let $\mathcal{M}$ be an oriented n-dimensional manifold with boundary $\partial\mathcal{M}$, and let $\tilde{\omega}$ be a differential $(n-1)$-form and $d\tilde{\omega}$ its exterior derivative, both defined on $\mathcal{M}$. Then:*

$$\int_{\mathcal{M}} d\tilde{\omega} = \int_{\partial\mathcal{M}} \tilde{\omega}. \tag{1.31}$$

1.3 Holonomies

In differential geometry, holonomy refers to the transformation a vector undergoes when it is parallel transported around a closed loop on a manifold. Due to the curvature of the manifold, the vector typically does not return to its original orientation, instead exhibiting a "torsion" that reflects the manifold's geometric properties.

Holonomy captures the curvature and geometric structure of a space, pointing out how local properties affect the behavior of objects transported along closed paths.

1.3.1 Parallel transport

It can easily be observed that, given how we defined vectors in subsection 1.1.2, in order to work with two or more vectors at once, we need to define them at the same point in the manifold, which means that we shall make clear how to carry a vector from a point to another "without changing its direction" [6]. This latter concept is known as *parallel transport.*
This is not trivial at all- try to think of doing this on a S^2 sphere, as shown in Fig.1.2-

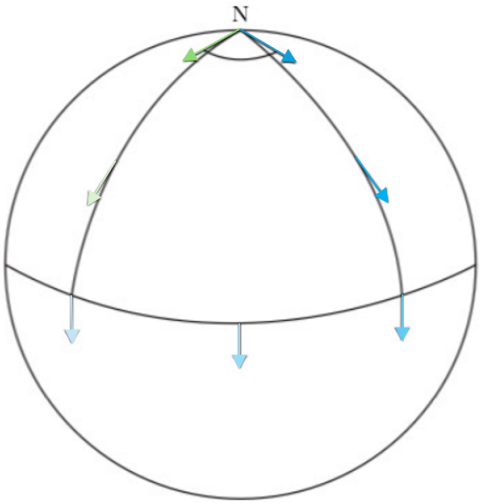

Fig. 1.2: Parallel transport around a closed loop on a sphere; at the same point N, after the transport, the vector appears different (not "parallel", at least with its usual meaning). Note how the colors vary. Image sourced from [10].

and embodies the main reason why a concept such as *affine connection* (see 1.3.2) is required.

Let $\mathcal{C} : (a, b) \to \mathcal{M}$ be a curve on the manifold $\mathcal{M}$ parameterized by λ and whose tangent vector field is $\bar{U} = d/d\lambda$. Consider then a point P on the curve and choose an arbitrary vector $\mathbf{V}_P \in T_P$. Our aim is to define a rule that allows us to parallel-transporting the vector $\mathbf{V}_P$ along $\mathcal{C}$. Hence, we will be able to define a derivative with respect to with the $\bar{V}$ field has zero rate change [6]. This mathematical object is called **covariant derivative** and is denoted by $\nabla_{\bar{U}}$.
Thus, a vector field $\bar{V}$ is said to be **parallel transported** along a curve $\mathcal{C}$ iff [7]:

$$\nabla_{\bar{U}} \bar{V} = 0 \quad \forall \lambda \in (a, b)\,. \tag{1.32}$$

Now, the covariant derivative is nothing but a derivative that can now be completely evaluated at the same point P, or, to be more precise, in the the tangent space T_P. Assuming $P = \mathcal{C}(\lambda_0)$, it takes the form [6]:

$$\nabla_{\bar{U}} \bar{V}\Big|_P = \lim_{\epsilon \to 0} \frac{\bar{V}_{\lambda_0+\epsilon}(\lambda_0) - \bar{V}(\lambda_0)}{\epsilon} \tag{1.33}$$

where $\bar{V}_{\lambda_0+\epsilon}$ refers to the vector field parallel transported to P.
It is clear that $\nabla_{\bar{U}}$ is not different from a differential operator from which it inherits the properties such as linearity and the Leibniz rule. In particular, provided that f is a scalar function:

$$\nabla_{\bar{U}}(f\bar{V}) = f\nabla_{\bar{U}}\bar{V} + \bar{V}\frac{df}{d\lambda}\,. \tag{1.34}$$

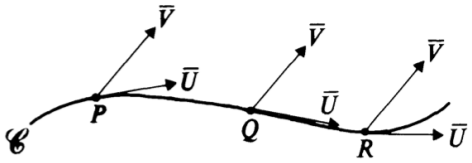

Fig. 1.3: The vector $\boldsymbol{V}_P$ is here parallel transported along $\mathcal{C}$: to each point of $\mathcal{C}$ it is possible to associate a vector of $\bar{V}$ (here, also denoted as $\bar{V}$) parallel to the starting vector $\boldsymbol{V}_P$. Image sourced from [6].

In addition, given g another scalar function defined on the manifold, the covariant derivative obeys [6]:

$$\nabla_{f\bar{U}+g\bar{W}}\bar{V} = f\nabla_{\bar{U}}\bar{V} + g\nabla_{\bar{W}}\bar{V}\,. \tag{1.35}$$

1.3.2 Affine connection

The covariant derivative derives from another significant concept: the affine connection. This essentially provides us with a rule for parallel transport, which otherwise wouldn't be uniquely defined.
The **affine connection** is mathematically represented by a map [7]:

$$\nabla : (\bar{U}, \bar{V}) \mapsto \nabla_{\bar{U}}\bar{V} \tag{1.36}$$

which transforms two vector fields in the correspondent covariant derivative- which is still a vector field.

Provided the manifolds we are working on is n-dimensional, we could still completely define the affine connection using the n^3 functions $\Gamma^{\lambda}{}_{\nu\mu}$ called **connection coefficients** [7] and also referred to as *Christoffel symbols*:

$$\nabla_\nu e_\mu \equiv \nabla_{e_\nu} e_\mu = e_\lambda \Gamma^{\lambda}{}_{\nu\mu}\,. \tag{1.37}$$

Here, $e_\nu \equiv \partial/\partial x^\nu$, $e_\mu \equiv \partial/\partial x^\mu$ denote the vector basis for $\bar{U}$ and $\bar{V}$ respectively, which means that $\bar{U} = U^\nu e_\nu$ and $\bar{V} = V^\mu e_\mu$. Knowing how they change, we can determine the behavior of the affine connection as a whole:

$$\nabla_{\bar{U}}\bar{V} = U^\nu \nabla e_\nu (V^\mu e_\mu) = U^\nu \left(\frac{\partial V^\lambda}{\partial x^\mu} + V^\nu \Gamma^{\lambda}{}_{\mu\nu} \right) e_\lambda \tag{1.38}$$

where we used the property shown in (1.34). Let us analyze the terms in the parentheses: the first one is the ordinal partial derivative of the component of the vector field, while the second one can be interpreted as a "geometric correction", allowing the preservation

of the parallelism.
As a matter of fact, the Christoffel symbols are responsible for the maintenance of the correctness of the covariant derivative, also under coordinates change. Given another set of coordinates $\partial/\partial y^\alpha$, they would change as [7]:

$$\widetilde{\Gamma}^\gamma_{\alpha\beta} = \frac{\partial x^\lambda}{\partial y^\alpha}\frac{\partial x^\mu}{\partial y^\beta}\frac{\partial y^\gamma}{\partial x^\nu}\Gamma^\nu_{\lambda\mu} + \frac{\partial^2 x^\nu}{\partial y^\alpha \partial y^\beta}\frac{\partial y^\gamma}{\partial x^\nu}\,. \tag{1.39}$$

1.3.3 Curvature

It is possible to associate to the connection the notion of **curvature**, which is the mathematical object which quantifies how the manifold $\mathcal{M}$ is curved, or, similarly, quantifies how the manifold deviates from being flat, namely how it differs from the Euclidean space.
In such case, the curvature can mathematically be expressed by the **Riemann curvature tensor** [7]:

$$\mathbf{R}(\bar{U},\bar{V},\bar{W}) = \nabla_{\bar{U}}\nabla_{\bar{V}}\bar{W} - \nabla_{\bar{V}}\nabla_{\bar{U}}\bar{W} - \nabla_{[\bar{U},\bar{V}]}\bar{W} \tag{1.40}$$

with $\bar{U},\bar{V},\bar{W}$ three arbitrary vector fields on $\mathcal{M}$.
It satisfies:

$$\mathbf{R}(\bar{U},\bar{V},W) = -\mathbf{R}(\bar{V},\bar{U},\bar{W})\,, \tag{1.41}$$

$$\mathbf{R}(\bar{U},\bar{V},\bar{W}) = U^\lambda V^\mu W^\nu \mathbf{R}(e_\lambda, e_\mu, e_\nu)\,. \tag{1.42}$$

The curvature tensor can also be expressed in terms of Christoffel symbols [7]:

$$R^\kappa{}_{\lambda\mu\nu} = \partial_\mu\Gamma^\kappa_{\nu\lambda} - \partial_\nu\Gamma^\kappa_{\mu\lambda} + \Gamma^\eta_{\nu\lambda}\Gamma^\kappa_{\mu\eta} - \Gamma^\eta_{\mu\lambda}\Gamma^\kappa_{\nu\eta}. \tag{1.43}$$

It is not difficult to see that the curvature tensor provides a measure of "how much" the vector $\bar{W}$ does differ when parallel transported along two different paths on the manifold [7]. In other words, we can say that the curvature determines the holonomy of the system.

1.4 Fiber bundles

Fiber bundles are mathematical structures that allow us to describe spaces with local product-like characteristics, but complex global properties.
These constructs are crucial for understanding the geometric and topological properties of physical systems, highlighting deep connections between local and global aspects.

We shall now introduce the concept.
A (differentiable) fiber bundle [7] is defined by a set of mathematical objects (E, B, π, F) such that:

- E, B, F are three differentiable manifolds, respectively called: **total space**, **base space** and **fiber**;

- π is a continuous surjection from the total to the base space $\pi : E \to B$ and is referred to as **bundle projection**. Its inverse $\pi^{-1}(P)$ is the **fiber *at*** P.
  The bundle projection π should always meet the following condition [11]: any $b \in B$ has a neighborhood U such that: $\varphi : \pi^{-1}(U) \to U \times F$ is a homeomorphism and $\text{proj}_U \circ \varphi = \pi\big|_{\pi^{-1}(U)}$, where $\text{proj}_U : U \times E \to U$ is the natural projection onto the U factor. Such φ are called **local trivializations** of the bundle.

Essentially, a fiber bundle is locally akin to the product space[9] $B \times F$ — even if it can be globally much more complex.
Usually, fibers bundle are denoted by the shorthand [7]: $E \xrightarrow{\pi} B$.

One of the most common examples of fiber bundles is the so-called *tangent bundle*, where the total space is obtained by combining a manifold $\mathcal{M}$ with the $T\mathcal{M}$ space, where:

$$T\mathcal{M} \equiv \bigsqcup_{P \in \mathcal{M}} T_P\mathcal{M} \,. \tag{1.44}$$

This type of fiber bundle is a **vector bundle**, i.e. a fiber bundle whose fiber is a vector space [7].

One useful tool when dealing with fiber bundles is the notion of a **cross section** (or just **section**), a smooth mapping from the base space into the total space of the bundle $s : B \to E$. This must clearly satisfy the condition that $\pi \circ s = id_B$ [7], that is, $\pi(s(b)) = b \ \forall b \in B$. When $s : U_i \to E$, with $U_i \in B$, we may talk of **local section**, as it is defined only within U_i and not all the base space.

1.4.1 Some examples: trivial and non trivial bundles

Fiber bundles that not only locally but also globally resemble the product of the base space and fiber $B \times F$ are called **trivial** fiber **bundles**, due to their intuitive and straightforward nature. More precisely, it means that there exists a local trivialization of E over the entire base space B and E itself is homeomorphic to the product space. When π is a smooth map that admits a smooth global trivialization, the fiber bundle is said to be *smoothly* trivial and E is diffeomorphic to $B \times F$: $E \simeq B \times F$ [12].

For instance, a cylinder and a torus can both be seen as trivial fiber bundles.
A cylinder C is the total space obtained as the product of a S^1 circle- acting as base space-

[9] Given two spaces X, Y their *product space* $X \times Y$ is the space made up of all the "ordered pairs" (x, y) such that $x \in X$ and $y \in Y$. If X, Y are manifolds, also $X \times Y$ is a manifold.

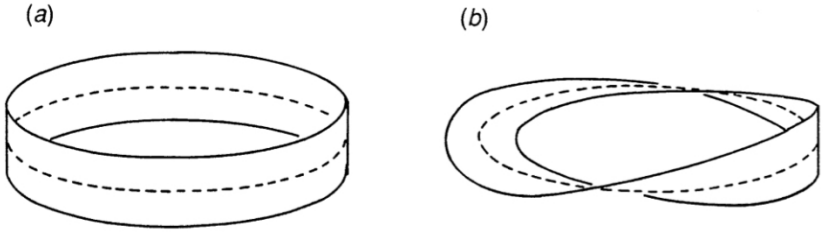

Fig. 1.4: Examples of fiber bundles: a cylinder (on the right, figure (a)) and a Möbius strip (on the right, figure (b)). In the latter, the fibres have been twisted. Note that in such cases the fibres $\mathbb{R}$ are actually intervals $I \subset \mathbb{R}$. Sourced from [6].

and $\mathbb{R}$- acting as fiber, meaning that fibers are infinitely-many vertical lines: $C = S^1 \times \mathbb{R}$. The bundle projection is defined as: $\pi : (\theta, x) \mapsto \theta$.
A 2-torus T^2 is the total space which can be instead obtained as: $T^2 : S^1 \times S^1$ with the bundle projection defined as: $\pi : (\theta_1, \theta_2) \mapsto \theta_1$.

We shall now return to the first example, the cylinder; we actually could have chosen to construct the total space differently [6], *twisting* the fibers. This would have given rise to a Möbius strip instead of a cylinder (see Fig.1.4).

1.4.2 Lie groups and algebra

Groups
Before digging into Lie groups we shall recall a more general definition for groups.
Let G be an algebraic structure with a defined *binary operation* $\cdot$ such that, given two elements $g_1, g_2 \in G$:

$$\cdot : (g_1, g_2) \mapsto g_1 \cdot g_2 \tag{1.45}$$

where $g_1 \cdot g_2 \in G$ (algebraic closure). This operation must have the following properties:

- it is associative: $(g_1 \cdot g_2) \cdot g_3 = g_1 \cdot (g_2 \cdot g_3), \quad \forall g_1, g_2, g_3 \in G$;
- there exists a *identity* or *unit element* $e \in G$ such that: $g \cdot e = e \cdot g = g, \quad \forall g \in G$;
- there exists an *inverse element* $g^{-1} \in G$ associated to any element $g \in G$ such that: $g \cdot g^{-1} = g^{-1} \cdot g = e$.

A group is said to be *Abelian* if the binary operation also satisfies the commutation law: $g_1 \cdot g_2 = g_2 \cdot g_1, \quad \forall g_1, g_2 \in G$.

A *homomorphism* between two groups is a map $h : G \to G'$ that preserves the binary operation, i.e.:

$$h(g_1 \cdot g_2) = h(g_1) \cdot h(g_2), \quad \forall g_1, g_2 \in G\,. \tag{1.46}$$

It is also possible to define the *generators* of the group G: given a subset $S \subset G$, this is said to be a *generating set* of G if each element of G can be written as a finite combination of element of S and their inverse.
A group is then called *cyclic* if it can be generated by a single element.

The dimension of a group depends on the dimension of its elements.

We are now ready to address Lie groups.
A **Lie group** is a differentiable manifold equipped with a group structure and such that the binary operation and the inverse operation[10] are differentiable [7].

Examples of Lie groups which are widely used in physical applications are the **general linear groups** $GL(n, K)$, representing all the possible invertible linear transformations on a n-dimensional vector space- defined on K. Their elements are $n \times n$ matrices and, usually, $K = \mathbb{R}$ or $K = \mathbb{C}$. The binary operation acts as the matrix multiplication, the inverse is just the matrix inverse [7].

It is also useful to mention and define some subgroups of $GL(n, K)$ -which are Lie groups themselves [7]: the **orthogonal group** $O(n)$, the **special linear group** $SL(n, K)$ and the **special orthogonal group** $SO(n)$:

$$O(n) = \{A \in GL(n, \mathbb{R}) \mid A^T A = \mathbb{I}\} \tag{1.47}$$

$$SL(n, K) = \{A \in GL(n, K) \mid \det(A) = 1\} \tag{1.48}$$

$$\begin{aligned} SO(n) &= \{A \in O(n) \mid \det(A) = 1\} \\ &= O(n) \cap SL(n, K). \end{aligned} \tag{1.49}$$

When $K = \mathbb{C}$, we can define the **unitary group** $U(n)$ and the **special unitary group** $SU(n)$:

$$U(n) = \{U \in GL(n, \mathbb{C}) \mid U^\dagger U = \mathbb{I}\} \tag{1.50}$$

$$\begin{aligned} SU(n) &= \{U \in U(n) \mid \det(U) = 1\} \\ &= U(n) \cap SL(n, \mathbb{C}). \end{aligned} \tag{1.51}$$

Note that ^{T} denotes the transposed matrix, while † denotes the Hermitian conjugate matrix.

Given two elements $a, g \in G$, with G a Lie group, we can define the **right** and **left transitions**, respectively denoted by R_a and L_a, as follows:

$$R_a g = g \cdot a \tag{1.52}$$

$$L_a g = a \cdot g \tag{1.53}$$

[10] The inverse operation is defined as: $^{-1} : g \mapsto g^{-1}$.

mapping from G to G.

Observation. Sometimes, for the sake of cleaner notation, we may omit the symbol $\cdot$ when denoting the binary operation of a group.

We will now discuss the properties of the left-translation only (for the right-translation the reasoning would be equivalent) [7].
The translation induces the map L_{g*}:

$$L_{g*} : T_h G \to T_{gh} G \tag{1.54}$$

which is a pushforward that maps a tangent vector at $h \in G$ to a tangent vector at $gh \in G$. A **left-invariant vector field** $\bar{V}$ on G is a vector field that satisfies:

$$L_{g*} \bar{V}|_h = \bar{V}|_{gh}. \tag{1.55}$$

The set of all left-invariant vector fields forms a **Lie algebra**, denoted by $\mathfrak{g}$. There is a natural isomorphism[11] between this Lie algebra $\mathfrak{g}$ and the tangent space at the identity element of G:

$$\mathfrak{g} \cong T_e G. \tag{1.56}$$

The **Lie bracket** of two elements[12] $T_\alpha, T_\beta \in \mathfrak{g}$ is a bilinear operation $[\ \ ,\ \ ] : \mathfrak{g} \times \mathfrak{g} \to \mathfrak{g}$ defined as:

$$[T_\alpha, T_\beta] = f^\gamma_{\alpha\beta} T_\gamma \tag{1.57}$$

where $f^\gamma_{\alpha\beta}$ are the *structure constants* of the Lie algebra, and $\{T_\alpha\}$ is a basis for $\mathfrak{g}$.

The **adjoint action** of G, denoted by Ad_g, is defined as:

$$\mathrm{Ad}_g(h) = ghg^{-1}, \quad \forall g, h \in G \tag{1.58}$$

The **differential** (tangent map) of the adjoint action at the identity element gives the **adjoint map**:

$$\mathrm{ad}_g : \mathfrak{g} \to \mathfrak{g}, \quad \mathrm{ad}_g(A) = gAg^{-1}, \quad \text{for } A \in \mathfrak{g}. \tag{1.59}$$

This map is called the **adjoint representation** of the Lie algebra, and it describes how elements of the Lie algebra transform under the conjugation action of the Lie group.

[11] A map between two sets $f : X \to Y$ is said to be an *isomorphism* if it is both one-one and surjective, that is it is possible to identify a one-to-one correspondence between X and Y.

[12] So far, we have used a specific notation—such as bold characters or bars—for vectors and vector fields. From now on, we will denote elements of the Lie algebra using symbols like T_α, as this is the conventional choice.

1.4.3 Principal fiber bundles

A **principal fiber bundle** is a fiber bundle whose fiber space coincides with its structure group.

The **structure group** G of a fiber bundle is a Lie group acting on F, which encodes some important structural information; more precisely, elements $t_i j \in G$ are such that, given two neighborhood $U_i, U_j \in F$ with $U_i \cup U_j \neq \varnothing$, $t_{ij} : U_i \cap U_j \to G$. These functions are called **transition functions** [7].

As an example, let us consider again the example of the cylinder and the Möbius strip (see Subsec.1.4.1). In this case, the difference lies in the structure group: in fact, for the cylinder, the transition functions are identity maps, whereas, in order to obtain the Möbius strip, they must be defined as: $t_1 2(\theta) : t \mapsto -t, \ \theta \in S^1$. Hence, the structure group of the cylinder is trivial, consisting of the only identity element $G^{(\text{cyl})} = \{e\}$, while the Möbius strip's one is made up of e together with another element g acting as: $g : t \mapsto -t$, $G^{(\text{Möb})} = \{e, g\}$.

Now, let us give a deeper look at the definition of principal fiber bundle: any fiber over a point P of the base space is a space isomorphic to G [13]. In mathematical terms this is expressed by:

$$\pi^{-1}(P) \cong U(1) \tag{1.60}$$

namely, an isomorphism between the fiber over each point of the base space and the $U(1)$ group.
This implies that the structure group G acts freely and transitively [7] on the fiber space F through **group actions**. A right (left) action of the group G on a point u of the principal bundle is defined as:

$$R_g(u) = u \cdot g \quad (L_g(u) = g \cdot u) \tag{1.61}$$

with $g \in G$. While this operation seems to be very similar to the already introduced right (left) transition, it is actually more general: it maps P in G, describing how the group act on the principal bundle- rather than on itself.

Principal fiber bundles are usually referred to with this notations: $P \xrightarrow{\pi} B$ or $P(B, G)$.

In the next subsection we will take care of providing a definition for connection, holonomy and curvature on principal fiber bundles.

1.4.4 Connection, holonomy and curvature on principal bundles

The concepts such as connection and curvature that we defined for manifolds, can be as well extended in a peculiar way to principal fiber bundles.

Consider a principal bundle and denote it with $P(B, G)$, where B is the base space and G the structure group and thus, by definition of principal bundle, its fiber space. Given $b \in B$ and $u \in P$, G_b is the fiber over $b = \pi(u)$. Eventually, T_uP is the tangent space of P, which is tangent to G_b at u.

Connection provides a way to separate T_uP into a **vertical subspace** V_uP and a **horizontal subspace** H_uP. These spaces are such that:

$$T_uP = V_uP \oplus H_uP \tag{1.62}$$

where $\oplus$ is the symbol for *direct sum*[13] between vector spaces.
More precisely, a connection on a principle bundle with such a purpose, is referred to as **connection one-form** (or, also, **Ehresmann connection**), which is a Lie-algebra-valued one-form $\tilde{\omega} \in \mathfrak{g} \otimes T^*P$[14] projecting T_uP onto V_uP [7]. The connection one-form must satisfy:

$$\tilde{\omega}(A^{\#}) = A, \quad \text{for } A \in \mathfrak{g} \tag{1.63}$$

$$R_g^*\tilde{\omega} = Ad_{g^{-1}}\tilde{\omega} \quad \text{for } g \in G \tag{1.64}$$

where:

$$A^{\#}f(u) = \frac{d}{dt}f(u\ \exp tA)|_t = 0 \quad \in V_uP \tag{1.65}$$

with f a smooth scalar function, is a vector tangent to P at u called *fundamental vector field* generated by A [7]. The mapping $\# : \mathfrak{g} \to V_uP$ is an isomorphism, $\mathfrak{g} \cong V_uP$, and defines the infinitesimal action of the Lie algebra $\mathfrak{g}$ on P.

In (1.64), R_g^* is the pullback of the one-form $\tilde{\omega}$ induced by the right action R_g.
Thus, for $\mathbf{V} \in T_uP$ [7]:

$$(R_g^*\tilde{\omega}_{ug})(\mathbf{V}) = \tilde{\omega}_{ug}(d\mathbf{V}) = g^{-1}\tilde{\omega}_u(\mathbf{V})g \tag{1.66}$$

where the subscripts ug, u specify where in the principal bundle the connection one-form is valued.

Eventually, we can also define the horizontal subspace as the *kernel* of $\tilde{\omega}$, that is [7]:

$$H_uP \equiv \{\mathbf{U} \in T_uP \mid \tilde{\omega}(\mathbf{U}) = 0\} \tag{1.67}$$

which follows directly the definition of the connection one-form.

[13] Given three vector spaces V, U, W, $V = U \oplus W$ means that $V = \{v = u + v | u \in U, w \in W\}$, where the sum $v = u + v$ must be unique, that is, $U \cap W = \varnothing$.

[14] T^*P is the dual bundle to the tangent bundle, the *cotangent bundle.*

Let us now define the **local connection form** $\mathcal{A}_i$ on U_i [7]:

$$\mathcal{A}_i \equiv \sigma_i^* \tilde{\omega} \quad \in \mathfrak{g} \otimes \Omega^1(U_i) \tag{1.68}$$

where σ_i^* is the pullback induced by the local section on U_i and $\Omega^1(U_i) \subset T^*P$.

On the other hand, given a family of local connection forms $\mathcal{A}_i$, we will be able to reconstruct the global connection $\tilde{\omega}$ by requiring that it satisfies [7]:

$$\sigma_i^* \tilde{\omega} = \mathcal{A}_i \quad \text{on } U_i. \tag{1.69}$$

Introducing the connection one-form, we mentioned the fact that it separates T_uP in V_uP and H_uP in such a way that the first one is the direct sum of the latter two spaces (1.62), i. e. the tangent space is uniquely decomposed. This implies that also $\tilde{\omega}$ should be unique. In order to satisfy such a request, any local form $\mathcal{A}_i$ should transform in a peculiar way- similar to that of the Christoffel symbols [7]:

$$\mathcal{A}_j = t_{ij}^{-1} \mathcal{A}_i t_{ij} + t_{ij}^{-1} dt_{ij} \tag{1.70}$$

where t_{ij} is the transition function dt_{ij} is its exterior derivative. Here, the first term represents the transformation of the local connection under action of the group, whereas the second term arises from the variation of the transition function itself.

Through the local connection form $\mathcal{A}_i$, we can provide a definition for parallel transport along a curve γ on a principal fiber bundle. Let us first introduce the notion of horizontal lifting, which will be necessary to define parallel transport.

Let $\gamma : [0,1] \to B$ be a curve on the base space. Another curve $\tilde{\gamma} : [0,1] \to P$ is the **horizontal lifting** of γ if $\pi \circ \tilde{\gamma} = \gamma$ and the tangent vector to $\tilde{\gamma}(t)$ belongs to $H_{\tilde{\gamma}(t)}P$. That is, any tangent vector $\tilde{\mathbf{V}}$ to $\tilde{\gamma}(t)$ is such that $\tilde{\omega}(\tilde{\mathbf{V}}) = 0 \ \forall t \in [0,1]$, which is an ordinary differential equation. Given that the lift can be written as:

$$\tilde{\gamma}(t) = \sigma_i(\gamma(t)) g_i(\gamma(t)) \tag{1.71}$$

with $g_i(\gamma(t)) \in G$, easy algebraic manipulations lead us to:

$$\begin{aligned} \frac{dg_i(t)}{dt} &= -\tilde{\omega}(\sigma_{i*}\mathbf{V}) g_i(t) \\ &= -\mathcal{A}_i(\mathbf{V}) g_i(t) \end{aligned} \tag{1.72}$$

where $g(t)$ is the short notation for $g(\gamma(t))$, while $\mathbf{V}$ is a tangent vector to $\gamma(t)$ at $\gamma(0)$ and it is such that $\tilde{V} = \tilde{\gamma}_* \mathbf{V}$. Note how the local form of the connection $\mathcal{A}$ is effectively involved in the definition of the parallel transport.

The fundamental theorem of ordinary differential equation ensures the local existence and uniqueness of a solution [7]. Thus, setting $g_i(0) = e$:

$$g_i(\gamma(t)) = \mathcal{P} \exp\left\{ -\int_0^1 \mathcal{A}_{i\mu} \frac{dx^\mu}{dt} dt \right\}. \tag{1.73}$$

Here, $\mathcal{P}$ is the path-ordering operator along $\gamma(t)$ (for more details, refer to section 10.1.4 in [7]).

Consider now a point $u_0 \in \pi^{-1}(\gamma(0))$ on the initial curve. From what has been discussed so far, there will be a unique point on the second curve, $u_1 = \tilde{\gamma}(1) \in \pi^{-1}(\gamma(1))$, obtained through the horizontal lift of $\gamma(t)$ called **parallel transport** of u_0 along the curve. In this way we can define a map: $\Gamma(\tilde{\gamma}) : \pi^{-1}(\gamma(0)) \to \pi^{-1}(\gamma(1))$ which maps u_0 onto u_1. This latter takes the following form [7]:

$$u_1 = \sigma_i(1) \mathcal{P} exp\left\{ -\int_0^1 \mathcal{A}_{i\mu} \frac{dx^\mu(\gamma(t))}{dt} dt \right\}. \tag{1.74}$$

It is convenient to define the so-called holonomy group, which is the subgroup of the structure group G in a principal fiber bundle $P(B, G)$, on which a connection $\tilde{\omega}$ is defined. To understand its role, consider the set of all the loops at $p = \pi(u)$, with $u \in P$: $C_p(B) = \{\gamma : [0, 1] \to B \mid \gamma(0) = \gamma(1) = p\}$. As mentioned, a loop γ essentially induces a transformation on the fiber of the following kind [7]:

$$\tau_\gamma : \pi^{-1}(p) \to \pi^{-1}(p) \tag{1.75}$$

such that:

$$\tau_\gamma(u \cdot g) = \tau_\gamma(u) \cdot g. \tag{1.76}$$

The **holonomy group** associated to the connection $\tilde{\omega}$ at u is then defined as [7]:

$$Hol_u(\tilde{\omega}) = \{g_\gamma \in G \mid \tau_\gamma(u) = u \cdot g_\gamma,\ \gamma \in C_p(B)\}. \tag{1.77}$$

That is, the holonomy group consists of the all transformations g_γ obtained by parallel transporting a point in the fiber $\pi^{-1}(p) = u$ along all possible closed loops γ based at that point.

We shall now generalize the concept of the covariant derivative to principal fiber bundles in order to define curvature. At the beginning of the subsection we saw how the connection $\tilde{\omega}$ decomposed the tangent space at the point u, T_uP, onto the two subspaces V_uP and H_uP. That is, each vector $\mathbf{V} \in T_uP$ will be also decomposed as: $\mathbf{V} = \mathbf{V}^V + \mathbf{V}^H$, with $\mathbf{V}^V \in V_uP$ and $\mathbf{V}^H \in H_uP$. The **covariant derivative** of a V-valued r-form on P, i. e. $\phi = \sum_{\alpha=1}^{k} \phi^\alpha \otimes e_\alpha \in \Omega^r(P) \otimes V$, with V k-dimensional vector space, takes the following form [7]:

$$D\phi(\mathbf{W}_1, ..., \mathbf{W}_{r+1}) \equiv d_P\phi(\mathbf{W}_1^H, ..., \mathbf{W}_{r+1}^H) \tag{1.78}$$

where the vectors $\mathbf{W}_1, ..., \mathbf{W}_{r+1} \in T_uP$ and $d_P\phi$ is the exterior derivative of ϕ on P.

Finally, curvature, that on a principal fiber bundle is called **curvature two-form** is expressed as [7]:

$$\Omega \equiv D\tilde{\omega} \quad \in \Omega^2(P) \otimes \mathfrak{g}. \tag{1.79}$$

The $\tilde{\omega}$ term clearly denotes the connection on the same bundle P.
The curvature satisfies:

$$R_g^*\Omega = g^{-1}\Omega g \quad \text{for } g \in G. \tag{1.80}$$

Connection one-form and curvature two-form on a principle bundle are related by the *Cartan's structure equation* which, given $\mathbf{V},\ \mathbf{U} \in T_uP$, reads as:

$$\Omega(\mathbf{V}, \mathbf{U}) = d_P\tilde{\omega}(\mathbf{V}, \mathbf{U}) + [\tilde{\omega}(\mathbf{V}), \tilde{\omega}(\mathbf{U})] \tag{1.81}$$

which can also be expressed as:

$$\Omega = d_P\tilde{\omega} + \tilde{\omega} \wedge \tilde{\omega}. \tag{1.82}$$

There also exists a theorem which establish the relationship between curvature two-form to the concept of holonomy: the *Ambrose-Singer theorem* [7].

Theorem. *Let $P(B, G)$ be a principal fiber bundle, then the Lie algebra $\mathfrak{h}_u$ associated to the holonomy group Hol_u of a point $u \in P$ is a subalgebra of $\mathfrak{g}$ spanned by:*

$$\Omega_u(\mathbf{V}, \mathbf{U}) \quad \textit{for } \mathbf{V}, \mathbf{U} \in H_uP. \tag{1.83}$$

To conclude the subsection, let us define the **local form $\mathcal{F}$ of the curvature two-form** Ω [7]:

$$\mathcal{F}_i \equiv \sigma_i^*\Omega \quad \in \mathfrak{g} \otimes \Omega^2(P). \tag{1.84}$$

Note the analogy between the latter and equation (1.68).
From the Cartan's structure equation (see (1.81), (1.82)) it is possible to derive the following form:

$$\mathcal{F}_i = d\mathcal{A}_i + \mathcal{A}_i \wedge \mathcal{A}_i \tag{1.85}$$

where d is the exterior derivative on the base space B.
Moreover, just as the local form of the connection, also the local form of the curvature should satisfy a certain condition in an overlap $U_i \cap U_j \in B$ [7]:

$$\mathcal{F}_j = t_{ij}^{-1}\mathcal{F}_i t_{ij}. \tag{1.86}$$

1.4.5 $U(1)$ bundles

A very significative principal fiber bundle in physical applications is the $U(1)$ bundle (think of Gauge theory [6], for instance).
The fibers of such a bundle are isomorphic to the group $U(1)$- that is, the structure group of the bundle is $U(1)$.

Let us recall the definition of the group right below:

$$U(1) = \{U \in GL(1, \mathbb{C}) \mid U^\dagger U = \mathbb{I}\}\,. \tag{1.87}$$

Elements of this group are unit complex numbers, that can be written as $g(\theta) = e^{i\theta} \in U(1),$ with $\theta \in [0, 2\pi)$. The binary operation is then multiplication of complex numbers, thus $U(1)$ group is Abelian.

By definition of Lie algebra (1.56), elements of $\mathfrak{u}(1)$ belongs to the $T_eU(1)$ space, meaning that $\mathfrak{u}(1) \in i\mathbb{R}$.

To clarify the relationship between this mathematical structure and the physical context of the next chapters, consider the following.

In quantum mechanics, any quantum state is only defined *up to* a global phase factor $e^{i\theta}$; this implies that, if $e^{i\theta}\,|\psi\rangle$ and $|\psi\rangle$ are two distinct mathematical states, the actual *observed* physics is the same, because measurable quantities are indeed unaffected by global phases.

A $U(1)$ bundle fits perfectly, as any fiber can be viewed as a complex line bundle (a one-dimensional complex vector space) where the points in the fiber correspond to states that differ only by a phase factor $e^{i\theta}$. These points all represent the same physical state.

We shall now discuss how connection and curvature are defined on a $U(1)$ bundle. Note that we shall omit the group's indices as the group is Abelian and one-dimensional, and we will set the structure constants at zero, $f^\gamma_{\alpha,\beta} = 0$ [7], which implies $[T, T] = 0$.
Based on what we have said so far, a $U(1)$ bundle can always *locally* be seen as the product space of the base space and the fiber space, i. e., $P|_U = U \times U(1),$ with $U \subset B$.
In such a framework, the local form of connection one-form can be written as [7]:

$$\mathcal{A} = \mathcal{A}_\mu dx^\mu \tag{1.88}$$

where $\mathcal{A}_\mu$ is a purely imaginary quantity since $\mathcal{A}$ is an element of the Lie algebra, x^μ are local coordinates on U and d the exterior derivative.
The local form of the curvature two-form is instead expressed as [7]:

$$\mathcal{F} = d\mathcal{A}. \tag{1.89}$$

The latter comes directly from the Cartan's structure equation (1.85), where $\mathcal{A} \wedge \mathcal{A} = 0$ as the group is Abelian. In components it appears as:

$$\mathcal{F}_{\mu\nu} = \partial_\mu \mathcal{A}_\nu - \partial_\nu \mathcal{A}_\mu \tag{1.90}$$

which can also be interpreted as a two-rank tensor.

Let us now focus on how these quantities do transform.
The transition functions are given by[15]:

$$t_{ij} : U_i \cup U_j \to U(1), \;\; t_{ij}(p) = e^{i\Lambda(p)}, \;\; \Lambda(p) \in \mathbb{R} \tag{1.91}$$

leading to the following reformulation of (1.70):

$$\mathcal{A}_j(p) = \mathcal{A}_i(p) + id\Lambda. \tag{1.92}$$

In components [7]:

$$\mathcal{A}_{j\mu} = \mathcal{A}_{i\mu} + i\partial_\mu \Lambda. \tag{1.93}$$

On the other hand, the local form of curvature, which originally transforms as (1.86), reduces in this context to:

$$\mathcal{F}_j = \mathcal{F}_i. \tag{1.94}$$

That is, curvature is invariant and thus can be considered globally defined.

The Hopf Bundle
The most common example of a non trivial $U(1)$ bundle is the Hopf bundle, named after the Swiss mathematician Heinz Hopf.
It is an algebraic structure widely used in physics, useful to describe different systems.

The base space of the bundle is a 2-sphere S^2 while the fibers are circles S^1. The total space is S^3, thus it is denoted as:

$$S^3 \xrightarrow{\pi} S^2. \tag{1.95}$$

Locally, we can consider S^3 as the product $S^3 = S^2 \times S^1$.
Visualizing such a structure—which exists in four dimensions—is not an easy task for us, as three-dimensional beings. A well-executed and intuitive attempt at this is illustrated in Fig.1.5.

The structure group is, as we have already mentioned, $U(1)$, indeed $S^1 \cong U(1)$. Hence, we shall consider $U(1)$ as fiber.

[15]Note that they are equivalent to gauge transformations.

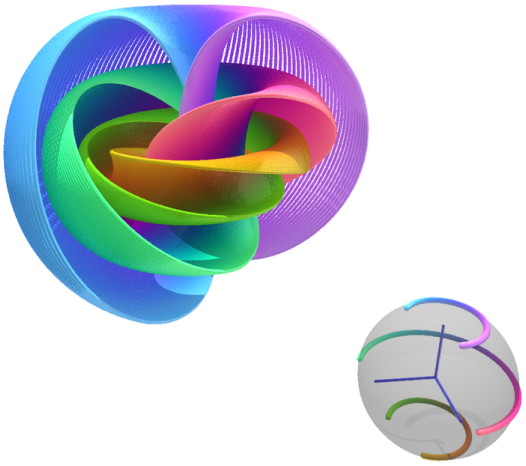

Fig. 1.5: A visual representation of the Hopf fibration, created by Professor Niles Johnson [14]. Note how the colors of the circles on the three-sphere (left) correspond to the colors of the arcs on the two-sphere (right).

Let us analyze the bundle.
The unit three-sphere is expressed through the following equation:

$$(x^1)^2 + (x^2)^2 + (x^3)^2 + (x^4)^2 = |z^0|^2 + |z^1|^2 = 1 \tag{1.96}$$

where z^0, z^1 are complex numbers: $z^0 = x^1 + ix^2$ and $z^1 = x^3 + ix^4$.
Analogously, the equation describing the unit two-sphere can be parametrized as:

$$(\xi^1)^2 + (\xi^2)^2 + (\xi^3)^2 = 1. \tag{1.97}$$

The bundle projection, also referred to as **Hopf map**, is thus defined as:

$$\begin{gathered} \pi : S^3 \to S^2 \\ \pi(x^1, x^2, x^3, x^4) = (2(x^1x^3 + x^2x^4), 2(x^2x^3 + x^1x^4), (x^1)^2 + (x^2)^2 - (x^3)^2 - (x^4)^2) \\ = (2\Re(z^0\bar{z^1}), 2\Im(z^0\bar{z^1}), |z^0|^2 - |z^1|^2) \end{gathered} \tag{1.98}$$

Consider now the stereographic projection coordinates[16] (X, Y) of a point in the southern hemisphere U_S of the two-sphere from the north pole. Let us consider the complex plane

[16] A stereographic projection is a map that projects points on the sphere (minus one point, typically the north or south pole) onto a plane. The plane can be, for instance, tangent to the sphere at the south pole or, as in this case, the plane containing the equator.

containing the hemisphere, on which we define $Z = X + iY$. It is possible to show that [7]:

$$Z = \frac{\xi^1 + ixi^2}{1 - \xi^3} = \frac{z^0}{z^1} \quad \text{with } \xi^i \in U_S, i = 1, 2, 3 \tag{1.99}$$

The same reasoning can be done for the points in the northern hemisphere. Given (U, V) the stereographic projection coordinates of the points of the northern hemisphere U_N from the south pole on a complex plane with the same characteristics as before, we can define $(W = U + iV)$:

$$W = \frac{\xi^1 - ixi^2}{1 + \xi^3} = \frac{z^1}{z^0} \quad \text{with } \xi^i \in U_N, i = 1, 2, 3 \tag{1.100}$$

Note that both Z and W are invariant if we transform z^0, z^1 with an element $g \in U(1)$:

$$(z^0, z^1) \mapsto (gz^0, gz^1) \tag{1.101}$$

and, also, that $Z = 1/W$ on $U_S \cap U_N$, namely, the equator.

Hence, local trivialization are differently defined for the southern and northern hemisphere. Respectively:

$$\begin{aligned} \varphi_S : \pi^{-1}(U_S) &\to U_S \times U(1) \\ (z^0, z^1) &\mapsto \left(\frac{z^0}{z^1}, \frac{z^1}{|z^1|} \right) \end{aligned} \tag{1.102}$$

$$\begin{aligned} \varphi_N : \pi^{-1}(U_N) &\to U_N \times U(1) \\ (z^0, z^1) &\mapsto \left(\frac{z^1}{z^0}, \frac{z^0}{|z^0|} \right) \end{aligned} \tag{1.103}$$

On the equator, $|z^0| = |z^1| = 1/\sqrt{2}$ and the local trivializations become:

$$\varphi_S : (z^0, z^1) \mapsto \left(\frac{z^0}{z^1}, \sqrt{2} z^1 \right) \tag{1.104}$$

$$\varphi_N : (z^0, z^1) \mapsto \left(\frac{z^1}{z^0}, \sqrt{2} z^0 \right) \tag{1.105}$$

while the transition function appears as:

$$t_{NS}(\xi) = \frac{\sqrt{2} z^0}{\sqrt{2} z^1} = \xi^1 + i\xi^2 \quad \in U(1). \tag{1.106}$$

For our purposes, we shall in addition mention the existence of an analogous structure, with a four-sphere S^4 as base space and a three-sphere S^3 as fiber space. The total space

will thus be a seven-sphere S^7 which locally resembles the product: $S^7 = S^4 \times S^3$. It is also referred to as Hopf bundle and denoted with:

$$S^7 \xrightarrow{\pi} S^4. \tag{1.107}$$

The structure group here is $SU(2)$, of which we recall the definition:

$$SU(2) = \{U \in U(2) \mid \det(U) = 1\}. \tag{1.108}$$

It is then of course possible to recognize $S^3 \cong SU(2)$, which is the reason why we can consider it a principle fiber bundle.
Eventually, the bundle projection involves *quaternionic* multiplication. An in-depth mathematical analysis will not follow here, but it can be found in [7], [15].

2 Geometric phases in quantum systems

In quantum systems, one can distinguish between two different types of phases:

- the *dynamical phase* $e^{-iEt/\hbar}$, which arises from the evolution of any stationary state of the system and depends on both energy and time;
- the *geometric phase* $e^{i\gamma}$, which instead depends only on the geometry of the path taken by the system in the parameter space.

The physical relevance of the first was already well-established when scientists started recognizing the significance of the latter as well.

In this chapter, we will focus on the most significant example of geometric phase: Berry's phase. We will then introduce key concepts such as Berry's connection and curvature, providing their mathematical interpretations. Eventually, some significative applications will be analyzed.

2.1 Berry's phase

Berry's phase and related concepts have proven to be highly significant in the geometric interpretation and understanding of various physical phenomena.

Historically speaking, S. Pancharatnam introduced and addressed the concept itself in his 1956 work on the theory of interference [16], but the first major breakthrough happened in 1984 with a paper by M. V. Berry [1].

2.1.1 Adiabatic theorem

The adiabatic theorem is fundamental in order to truly understand what is the physical reason behind the geometric phase.

The theorem, as it was firstly introduced by M. Born and V. Fock [17] in 1928, sates that:

Theorem. *A physical system remains in its instantaneous eigenstate if a given perturbation is acting on it slowly enough and if there is a gap between the eigenvalue and the rest of the Hamiltonian's spectrum.*

Proof. (Note that, from now on, we shall use the Dirac notation.)

Let the $|n(t)\rangle$ be the eigenstates of a time-dependent Hamiltonian $\hat{H}(t)$, so that:

$$\hat{H}(t)\,|n(t)\rangle = E_n(t)\,|n(t)\rangle \tag{2.1}$$

for any time t, where $E_n(t)$ are the instantaneous eigenvalues, say the energies that characterize the n-th instantaneous eigenstate $|n(t)\rangle$.
The time evolution of a state associated to the Hamiltonian $\hat{H}(t)$, denoted by $|\psi(t)\rangle$, is governed by the time-dependent Schrödinger equation:

$$\hat{H}(t)\,|\psi(t)\rangle = i\hbar\,|\dot{\psi}(t)\rangle \tag{2.2}$$

which can be re-written as:

$$i\hbar\sum_n \dot{c_n}(t)\,|n(t)\rangle + i\hbar\sum_n c_n(t)\,|\dot{n}(t)\rangle = \sum_n c_n(t)\hat{H}(t)\,|n(t)\rangle \tag{2.3}$$

taking into account that any state, at any time, can be expanded in the basis made up of the eigenstates:

$$|\psi(t)\rangle = \sum_n c_n(t)\,|n(t)\rangle \tag{2.4}$$

where $c_n(t)$ are the time dependent coefficients.
Using (2.1) in (2.3) and muliplying both sides for $\langle m(t)|$[1],it is possible to derive the time evolution of the coefficients appearing in (2.4):

$$\dot{c_m}(t) = \frac{i}{\hbar}c_m(t)E_m(t) - \sum_n c_n(t)\,\langle m(t)|\dot{n}(t)\rangle \tag{2.5}$$

Let us now focus on the meaning of $\langle m(t)|\dot{n}(t)\rangle$ when $m \neq n$. By differentiating with respect to time (2.1) and multiplying by $\langle m(t)|$, the equation takes the following form:

$$\langle m(t)|\dot{n}(t)\rangle = -\frac{\langle m(t)|\,\dot{\hat{H}}\,|n(t)\rangle}{E_m(t) - E_n(t)} \tag{2.6}$$

If the hypothesis of slow transformation and (finite) gap between eigenvalues- which means $E_m(t) - E_n(t) \neq 0, \forall t$- helds, this term is negligible, so that (2.5) takes the form:

$$\dot{c_m} = i\left(\frac{E_m(t)}{\hbar} + i\,\langle m(t)|\dot{m}(t)\rangle\right)c_m(t) \tag{2.7}$$

[1] $|m(t)\rangle$ is an arbitrary eigenstate and both $m = n$ and $m \neq n$ (with $\langle m(t)|n(t)\rangle = \delta_{mn}$) are possible.

Finally, we can integrate and find [18]:

$$c_n(t) = c_n(0)e^{i\theta_n(t)}e^{i\gamma_n(t)} \tag{2.8}$$

where:

$$\theta_n(t) = -\frac{1}{\hbar}\int_0^t E_n(t')dt' \tag{2.9}$$

is the dynamical phase, while:

$$\gamma_n(t) = i\int_0^t \langle n(t')|\dot{n}(t')\rangle\, dt' \tag{2.10}$$

is the geometric phase.
It is possible to show that θ and γ are both purely real.
For the dynamical phase, it is trivial and quite intuitive as $\theta_n(t)$ is the integral of an energy, which is real by definition.
With regard to the geometric phase, we shall prove that the bra-ket produt is purely imaginary;

$$\frac{d}{dt}\langle m(t)|m(t)\rangle = 0 \tag{2.11}$$

as we know that the inner product of an eigenstate with itself equals always to one. At the same time, we can compute:

$$\langle \dot{m}(t)|m(t)\rangle + \langle m(t)|\dot{m}(t)\rangle = \langle m(t)|\dot{m}(t)\rangle^* + \langle m(t)|\dot{m}(t)\rangle = 2\Re\langle m(t)|\dot{m}(t)\rangle \tag{2.12}$$

This eventually leads to:

$$\Re\langle m(t)|\dot{m}(t)\rangle = 0 \tag{2.13}$$

which validates our hypothesis.
This guarantees that $|c_n(t)|^2 = |c_n(0)|^2$.

The latter observation completes our discussion since it means that if the system is in an eigenstate $|n(0)\rangle$ of $\hat{H}(0)$ at t=0, the time when the transformation begins, it remains in an instantaneous eigenstate of $\hat{H}(t)$, for any t, up to a phase factor [19]:

$$|\psi_n(t)\rangle = \sum_n c_n(t)\,|n(t)\rangle = e^{i\theta_n(t)}e^{i\gamma_n(t)}\,|n(t)\rangle \tag{2.14}$$

during the whole evolution. □

Observation. If the instantaneous eigenstates $|n(t)\rangle$ are real, the geometric phase $\gamma_n(t)$ vanishes, as the only way for $\gamma_n(t)$ to be real is $\langle n(t)|\dot{n}(t)\rangle$ to be purely imaginary.

Remark. Equation (2.14) could actually be written in a more rigorous way, i.e.:

$$|\psi_n(t)\rangle \simeq e^{i\theta_n(t)}e^{i\gamma_n(t)}\,|n(t)\rangle \tag{2.15}$$

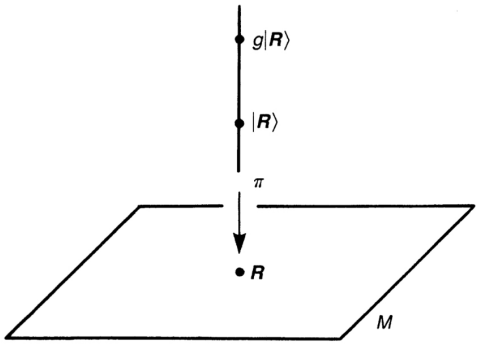

Fig. 2.1: Intuitive visualizing of the $U(1)$ bundle as described in the text. The n index is not used as we are effectively considering only the nth eigenstate. Sourced from [7].

Indeed, the theorem could also be stated[2] as [20]:

$$||\psi_{n,real}(t) - \psi_{n,adiabatic}(t)|| \leq \frac{constant}{T} \quad \forall t \in]0, T[\tag{2.16}$$

where $\psi_{n,real}(t)$ is the exact solution of the final state of the system, $\psi_{n,adiabatic}(t)$ is the right-hand member of (2.15), T is the duration of the transformation, *constant* is a scalar depending on ΔE.
It is immediate to note that the approximate solution is closer to the real one when T is large — at least, as long as the constant, i. e. ΔE, does not vanish.

2.1.2 Berry's phase

In this subsection, we will provide a complete definition of Berry's phase and then proceed with some observations that will lead us to the concepts of Berry's connection and curvature, both discussed in the next two subsections.

Consider now the set of parameters on which the system under examination depends, denoted as N parameters. These make up the coordinates of a vector $\mathbf{R} = (R_1, R_2, ..., R_N)$ in a N-dimensional manifold [7] referred to as parameter space.

The Hamiltonian associated to the system for any time t is a function of the parameters: $\hat{H}(\mathbf{R}(t))$.

Remark. For our purposes, the most suitable structure we can consider is a $U(1)$ bundle [21] (see Subsec.1.4.5). Parameter space represents the base space, while the fibers over each $\mathbf{R}$ are copies of the unitary group $U(1)$. Namely:

$$\pi^{-1}(\mathbf{R}) \cong U(1). \tag{2.17}$$

[2]By definition, the norm of an arbitrary $|\phi\rangle$ in a Hilbert space is: $||\phi|| = \sqrt{\langle\phi|\phi\rangle}$

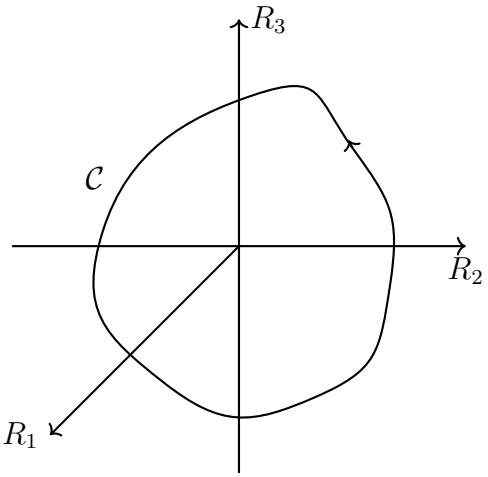

Fig. 2.2: An example of a cycle visualized in a three-dimensional parameter space.

This implies that any state of the system belongs to an *equivalence class*:

$$[|n(\mathbf{R})\rangle] \equiv \{e^{i\theta} |n(\mathbf{R})\rangle \mid e^{i\theta} \in U(1)\} \tag{2.18}$$

and it can be denoted with it. The bundle projector will thus be defined as:

$$\pi(e^{i\theta} |n(\mathbf{R})\rangle) = \mathbf{R}. \tag{2.19}$$

These concepts are summarized in the illustration in Fig.2.1.

Suppose the system is initially in a stationary state at $t = 0$ and the parameters $\mathbf{R}$ slowly changing over time. The evolution ends at time $t = T$ such that $\mathbf{R}(0) = \mathbf{R}(T)$, with T being sufficiently large to justify the use of the adiabatic approximation (see 2.1.1). In the parameter space, this evolution traces out a closed path $\mathcal{C}(t)$. An example is shown in Fig. 2.2.

Assuming any choice of the phases for the eigenstates $|n(\mathbf{R}(t))\rangle$ differentiable and such that the function remains single-valued for a whole domain in the parameters space that includes $\mathcal{C}$, and given that the adiabatic approximation is applicable, it is straightforward to find an expression for an arbitrary system's instantaneous state $|\psi(t)\rangle$ [1]. From the Adiabatic Theorem we are able to write:

$$|\psi(t)\rangle = e^{i\theta_n(t)} e^{i\gamma_n(t)} |n(\mathbf{R}(t))\rangle \tag{2.20}$$

where:

$$\theta_n(t) = \frac{-1}{\hbar} \int_0^T E_n(\mathbf{R}(t'))\, dt' \tag{2.21}$$

is the dynamical phase, while:

$$\gamma_n(t) = i \int_0^T \langle n(\mathbf{R}(t'))|\dot{n}(\mathbf{R}(t')\rangle \tag{2.22}$$

is the geometric phase. Whenever $\mathbf{R}(0) = \mathbf{R}(T)$, — and the expression fails to vanish — as in the case here, the latter takes the name of Berry's phase.

We shall now find a better form to express equation (2.22) in order to highlight its properties.
Inserting (2.20) in the Schrödinger equation — analogous to (2.2) — leads us to:

$$\dot{\gamma}_n(t) = i \langle n(\mathbf{R}(t))|\nabla_{\mathbf{R}}\, n(\mathbf{R}(t))\rangle \cdot \dot{\mathbf{R}}(t) \tag{2.23}$$

The next step is crucial since it embodies the core of the discussion.
Indeed, we are now able to write the geometrical phase change along the closed path $\mathcal{C}$ as [1]:

$$\gamma_n(\mathcal{C}) = i \oint_{\mathcal{C}} \langle n(\mathbf{R})|\nabla_{\mathbf{R}}\, n(\mathbf{R})\rangle \cdot d\mathbf{R} \tag{2.24}$$

This means that Berry's phase is entirely defined by the parameter space and does not depend on time. It is a function of the path that the system traverses in such space, while it is independent of how long it takes.

Observation. If the parameter space is 1D, Berry's phase will automatically vanish.

2.1.3 Berry's connection

The integrand of (2.24) represents an interesting physical quantity, called Berry's connection and denoted by $\mathcal{A}_n(\mathbf{R})$:

$$\mathcal{A}_n(\mathbf{R}) = \langle n(\mathbf{R})|\nabla_{\mathbf{R}}\, n(\mathbf{R})\rangle \tag{2.25}$$

It is a vector-valued function (N components, one for each parameter: the vector structure come from the gradient in parameter space), that is a one-form, in the parameter space. Namely, it is an example of a local form of the connection one-form on a $U(1)$ bundle.

Berry's phase can be re-written with respect to it as:

$$\gamma_n(\mathcal{C}) = i \oint_{\mathcal{C}} \mathcal{A}_n(\mathbf{R}) \cdot d\mathbf{R} \tag{2.26}$$

The interesting aspect of $\mathcal{A}_n(\mathbf{R})$ lies in its behavior when considering:

$$|n'(\mathbf{R})\rangle = e^{-i\beta(\mathbf{R})}\, |n(\mathbf{R})\rangle \qquad \beta \in \mathbb{R} \tag{2.27}$$

which is still an eigenstate of the Hamiltonian of the system since it is known that they can be chosen up to a phase. Note that we essentially just used the action of the group $U(1)$, and that $|n'(\mathbf{R})\rangle, |n(\mathbf{R})\rangle \in [|n(\mathbf{R})\rangle]$, that is, they belong to the same fiber.
We can compute $\mathcal{A}'_n(\mathbf{R})$:

$$\mathcal{A}'_n(\mathbf{R}) = \langle n'(\mathbf{R})|\nabla_{\mathbf{R}}\, n'(\mathbf{R})\rangle = \langle n(\mathbf{R})|e^{i\beta(\mathbf{R})}\,\nabla_{\mathbf{R}}\, e^{-i\beta(\mathbf{R})}|n(\mathbf{R})\rangle \tag{2.28}$$

which, for the fact that the gradient $\nabla_{\mathbf{R}}$ acts on everything to the right, becomes:

$$\mathcal{A}'_n(\mathbf{R}) = \mathcal{A}_n(\mathbf{R}) + i\nabla_{\mathbf{R}}\,\beta(\mathbf{R}) \tag{2.29}$$

Fundamentally, it has just been shown that the Berry's connection behaves in parameter space much like the vector potential does in phase space: it transforms with the gradient of a function [22].
As a matter of fact, equation (2.29) is entirely equivalent to a gauge transformation of the vector potential in an electromagnetic field:

$$\mathbf{A}' = \mathbf{A} + i\nabla\Phi \tag{2.30}$$

where $\mathbf{A}$ is the vector potential, while $\Phi(t, \mathbf{x})$ is an arbitrary gauge function. Indeed, gauge formalism lends itself to being analyzed in the context of $U(1)$ formalism[3].
Hence, this quantity is sometimes referred to as "Berry's potential".

We are thus not surprise to see the similarity with the compatibility requested to the local form of the connection one-form on a principle fiber bundle (1.92).

Let us now reflect on the concept of connection. Referring back to our discussion on the affine connection in 1.3.2, we can recall that the latter is characterized by the Christoffel symbols, which ensure the correct form of the covariant derivative by transforming appropriately under a change of coordinates and preserving parallel transport in the tangent space.

On the other hand, Berry's connection also transforms in a way that depends on the coordinate change, but its purpose is to "preserve the gradient under a gauge transformation" [6] in the parameter space.

Thus, both connections adjust in order to preserve a specific property: the affine connection maintains parallelism, while Berry's connection ensures the consistency of the quantum phase. In this way, Berry's connection guarantees a well-defined Berry's phase (see (2.31), (2.32)).

Remark. Further reasoning [2] by B. M. Simon in 1983, already addressed the fact that

[3]In this case, the $U(1)$ bundle is trivial, namely $P = \mathbb{R}^4 \times U(1)$ [7].

adiabatic theory would provide a rule for transporting the eigenstate $|n(\mathbf{R})\rangle$ along $\mathcal{C}$. This rule indeed corresponds to the connection (2.26) on the bundle[4]. This interpretation suggests that Berry's phase can be viewed as an associated holonomy [7].
See Subsec.2.1.5 for a more in-depth analysis.

We shall now compute the effects of (2.27) on Berry's phase itself:

$$\begin{aligned}\gamma'_n(\mathcal{C}) = \oint_{\mathcal{C}} \mathcal{A}'_n(\mathbf{R}) \cdot d\mathbf{R} &= \oint_{\mathcal{C}} [\mathcal{A}_n(\mathbf{R}) + \nabla_{\mathbf{R}}\, \beta(\mathbf{R})] \cdot d\mathbf{R} \\ &= \gamma_n(\mathcal{C}) + \beta(\mathbf{R}_f) - \beta(\mathbf{R}_i)\end{aligned} \tag{2.31}$$

where $\mathbf{R}_i$ is the point in the parameter space where the evolution starts while $\mathbf{R}_f$ where it ends.
Recalling that, for Berry's phase $\mathbf{R}_i = \mathbf{R}_f$, we conclude that:

$$\gamma'_n(\mathcal{C}) = \gamma_n(\mathcal{C}) \tag{2.32}$$

which means that Berry's phase is gauge-invariant, therefore observable [22].

Global form of the connection one-form

The fact that $\mathcal{A}_n$ is not a *global* connection arises already from the parallelism with the local form we studied in Sec.1.4. It can actually be shown that there exists a unique global connection one-form $\tilde{\mathcal{A}}$ over the $U(1)$ bundle in question. Given $u \in P$, i. e., the total bundle, [23]:

$$\tilde{\mathcal{A}} \equiv \mathcal{A} - i\frac{d_P u}{u} \tag{2.33}$$

where d_P is the exterior derivative on the total bundle P. Equation (2.33) is, indeed, gauge invariant.

As pointed out in the already mentioned Sec.1.4, the global connection $\tilde{\mathcal{A}}$ can be reduced to the local form $\mathcal{A}_i$ on an arbitrary chart U_i through the pullback of $\tilde{\mathcal{A}}$ induced by the local section (see (1.69)).

2.1.4 Berry's curvature

Another important concept is Berry's curvature. It arises from the fact that evaluating equation (2.24) can be quite demanding.
The procedure could become simpler by transforming the contour integral into a surface integral, i.e., an integral over any surface whose boundary corresponds to $\mathcal{C}$.

[4]Actually, B. M. Simon considered a slightly different fiber bundle, where the fibers were the eigenspaces, but the very first intuition that Berry's phase is the expression of a holonomy was his.

In a three-dimensional parameter space, this can be accomplished applying Stokes's theorem:

$$i \oint_{\mathcal{C}} \langle n(\mathbf{R})|\nabla_{\mathbf{R}}\, n(\mathbf{R})\rangle \cdot d\mathbf{R} = -\Im \iint_{\Sigma(\mathcal{C})} \nabla_{\mathbf{R}} \times \langle n(\mathbf{R})|\nabla_{\mathbf{R}}\, n(\mathbf{R})\rangle \cdot d\mathbf{S} \tag{2.34}$$

where $d\mathbf{S}$ represents the infinitesimal surface element in the parameter space, $\Sigma(\mathcal{C})$ the surface itself. The fact that we are only interested in the imaginary part of this term can be explained by recalling that the bra-ket product appearing in the geometric phase (2.24) is purely imaginary.
The integrand quantity on the right-hand side is what we call Berry's curvature, denoted by $\mathcal{V}_n(\mathbf{R})$:

$$\mathcal{V}_n(\mathbf{R}) = \Im\left[\nabla_{\mathbf{R}} \times \langle n(\mathbf{R})|\nabla_{\mathbf{R}}\, n(\mathbf{R})\rangle\right] \tag{2.35}$$

which can also be expressed, in a more common way, with respect to Berry's connection as:

$$\mathcal{V}_n(\mathbf{R}) = \nabla_{\mathbf{R}} \times \mathcal{A}_n(\mathbf{R}) \tag{2.36}$$

From (2.36) and (2.29), it is natural to identify an analogy with the magnetic field; Berry's curvature $\mathcal{V}_n(\mathbf{R})$ is consistent with a magnetic field in the parameter space whose vector potential is $\mathcal{A}_n$.

Berry's phase can of course be written also with respect to $\mathcal{V}_n(\mathbf{R})$ in the form:

$$\gamma_n(\mathcal{C}) = -\iint_{\Sigma(\mathcal{C})} \mathcal{V}_n(\mathbf{R}) \cdot d\mathbf{S} \tag{2.37}$$

from which we can better understand the physical meaning of $\mathcal{V}_n(\mathbf{R})$: its flux is Berry's phase [24].

Now, equation (2.35) can be manipulated by first applying the identity $\nabla \times (\mathbf{A} \cdot \mathbf{B}) = (\nabla \mathbf{A}) \cdot \mathbf{B} - \mathbf{A} \cdot (\nabla \mathbf{B})$ and then using the completeness relation[5]:

$$\mathcal{V}_n(\mathbf{R}) = \Im \sum_{m \neq n} \langle \nabla_{\mathbf{R}} n(\mathbf{R})|m(\mathbf{R})\rangle \times \langle m(\mathbf{R})|\nabla_{\mathbf{R}} n(\mathbf{R})\rangle \tag{2.38}$$

where the case $m = n$ is excluded because of the purely imaginary nature of $\langle n|\nabla n\rangle$ -which would lead to a cross product $\langle n|\nabla n\rangle \times \langle \nabla n|n\rangle$ purely real.
In the same way we previously computed (2.6), we can obtain a new form for the off-diagonal terms:

$$\langle m(\mathbf{R})|\nabla_{\mathbf{R}} n(\mathbf{R})\rangle = \frac{\langle m(\mathbf{R})|\, \nabla_{\mathbf{R}} \hat{H}(\mathbf{R})\, |n(\mathbf{R})\rangle}{E_n(\mathbf{R}) - E_m(\mathbf{R})} \tag{2.39}$$

[5] $\sum_n |n\rangle \langle n|\, dn = \mathbb{I}$ which holds for any $|n\rangle$ eigenstate

which allows us to re-express (2.38) in the following form:

$$\mathcal{V}_n(\mathbf{R}) = \Im \sum_{m \neq n} \frac{\langle n(\mathbf{R})| \nabla_{\mathbf{R}} \hat{H}(\mathbf{R}) |m(\mathbf{R})\rangle \times \langle m(\mathbf{R})| \nabla_{\mathbf{R}} \hat{H}(\mathbf{R}) |n(\mathbf{R})\rangle}{(E_n(\mathbf{R}) - E_m(\mathbf{R}))^2} \,. \tag{2.40}$$

What is really significant here is to note how we managed to eliminate the $|\nabla_{\mathbf{R}} n(\mathbf{R})\rangle$ terms. These were indeed the terms that constrained the choice of phase for the eigenstates. Now we discover that Berry's phase is not even dependant on phase relations between eigenstates with different parameters and the eigenstates no longer need to be single-valued in the parameter space [1].
In a sense, we arrived at the same conclusion as in (2.32).

For completeness, we now address how the latter discussion extends to cases where the parameter space has a dimension greater than two (for an in-depth discussion, refer to [25]). There exists indeed a generalization of the Stokes's theorem— stated in the previous chapter (1.31)—which takes (2.24) and transforms it into an integral of a two-form over any surface spanning $\mathcal{C}$ in parameter space [1], just like it happens in three dimensions (see (2.37)). The two-form can be written as:

$$\begin{aligned} \mathcal{V}_n(\mathbf{R}) &= \Im \sum_{m \neq n} \frac{\langle n(\mathbf{R})| \frac{d\hat{H}(\mathbf{R})}{d\mathbf{R}} |m(\mathbf{R})\rangle \wedge \langle m(\mathbf{R})| \frac{d\hat{H}(\mathbf{R})}{d\mathbf{R}} |n(\mathbf{R})\rangle}{(E_n(\mathbf{R}) - E_m(\mathbf{R}))^2} \\ &= \Im \sum_{m \neq n} \frac{\langle n(\mathbf{R})|\partial_\mu \hat{H}(\mathbf{R})|m(\mathbf{R})\rangle \langle m(\mathbf{R})|\partial_\nu \hat{H}(\mathbf{R})|n(\mathbf{R})\rangle}{(E_n(\mathbf{R}) - E_m(\mathbf{R}))^2} \, dR^\mu \wedge dR^\nu \end{aligned} \tag{2.41}$$

whose component form is actually equivalent to an anti-symmetric second rank tensor (as we already stated with (1.90)):

$$\mathcal{V}_{n,\mu\nu}(\mathbf{R}) = \frac{\partial}{\partial R^\mu} \mathcal{A}_{n,\nu}(\mathbf{R}) - \frac{\partial}{\partial R^\nu} \mathcal{A}_{n,\mu}(\mathbf{R}). \tag{2.42}$$

By the definition of the local form of the curvature on a $U(1)$ bundle (1.89), we are able to derive this equivalence between Berry's curvature and connection:

$$\mathcal{V}_n(\mathbf{R}) = -d\mathcal{A}_n(\mathbf{R}) \,. \tag{2.43}$$

Here, $d\mathcal{A}_n(\mathbf{R})$ is the exterior derivative of $\mathcal{A}_n(\mathbf{R})$ on the $U(1)$ bundle. The minus is purely conventional. As a confirmation, latter equation also aligns with what we expect from the generalized Stokes' theorem (1.31).

An alternative expression for Berry's curvature that highlights its anti-symmetric nature is [23]:

$$\mathcal{V}_n(\mathbf{R}) = \frac{1}{2} \left\{ \left\langle \frac{\partial |n(\mathbf{R})\rangle}{\partial R^i} \middle| \frac{\partial |n(\mathbf{R})\rangle}{\partial R^j} \right\rangle - \left\langle \frac{\partial |n(\mathbf{R})\rangle}{\partial R^j} \middle| \frac{\partial |n(\mathbf{R})\rangle}{\partial R^i} \right\rangle \right\} dR^i \wedge dR^j. \tag{2.44}$$

Berry's curvature, like Berry's phase, it's gauge-invariant, as we have already seen for an arbitrary curvature two-forms on $U(1)$ bundles (see (1.94)). Hence, it is a globally defined quantity in the parameter space. Nonetheless, it offers a local characterization of the geometric properties of the parameter space [26].

Remark. B. M. Simon [2] suggested a different form to express the curvature, stressing that the one chosen by M. V. Berry (2.41) might mislead the reader into thinking that it depends on specific details of the Hamiltonian rather than on its eigenspaces. The two-form should therefore be written as:

$$\mathcal{V}_n = \Im \sum_{i<j} \left\langle \frac{\partial \left| n(\mathbf{R}) \right\rangle}{\partial R^i}, \frac{\partial \left| n(\mathbf{R}) \right\rangle}{\partial R^j} \right\rangle dR^i \wedge dR^j \,. \tag{2.45}$$

2.1.5 Holonomy interpretation of Berry's phase

This will be the subsection concluding — as we will be showing it — the discussion about the interpretation of Berry's phase as a holonomy associated with the connection $\mathcal{A}$ on the $U(1)$ bundle over the parameter space.

This time, we shall consider a modified Hamiltonian $\hat{\mathcal{H}}(\mathbf{R})$ in order to remove the dynamical phase from our discussion [2]:

$$\hat{\mathcal{H}}(\mathbf{R}) \equiv \hat{H}(\mathbf{R}) - E_n(\mathbf{R}). \tag{2.46}$$

In this way, the n-th eigenstate $|n(\mathbf{R})\rangle$ will coincide with the zero-energy state.
The solution of the Schrödinger equation will thus be [7]:

$$|\psi(\mathbf{R}(t))\rangle = e^{i\gamma_n(t)} \left| n(\mathbf{R}(t)) \right\rangle \tag{2.47}$$

where the only phase factor is the geometric one, whose $\gamma_n(t)$ is given by (2.22).

A loop in a subspace $U \subset \mathbf{R}$-space[6] is defined as: $\mathcal{C} : [0, T] \to B$, where the base space is the parameter space, indeed. A section σ on the chart U is [7]:

$$\sigma : \mathbf{R}(t) \mapsto \left| n(\mathbf{R}(t)) \right\rangle . \tag{2.48}$$

From (1.71), we shall define an horizontal lifting also in this very framework such as:

$$\tilde{\mathbf{R}}(t) = \sigma(\mathbf{R}(t)) g(\mathbf{R}(t)) \tag{2.49}$$

with $g(\mathbf{R}(t)) \in U(1)$ and $g(\mathbf{R}(0)) = 1$ corresponds to the unit element.
Using (1.72), we can understand how an arbitrary $g(\mathbf{R}(t))$ evolves through t:

$$\frac{dg(t)}{dt} g(t)^{-1} = -\mathcal{A}_n \left(\frac{d}{dt} \right) = - \left\langle n(\mathbf{R}(t)) \right| \frac{d}{dt} \left| n(\mathbf{R}(t)) \right\rangle \tag{2.50}$$

[6] $\mathbf{R}$-space is just another name for the parameter space.

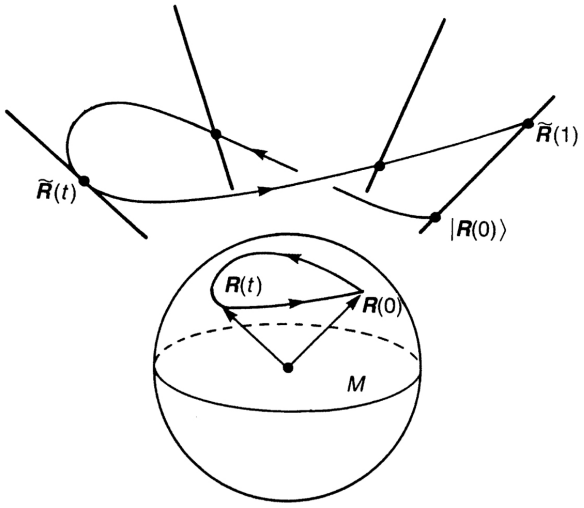

Fig. 2.3: A visual representation of the procedure we described in the text. Here, the base space, namely the parameter space, is denoted by M, and, again, The n index is not used as we are effectively considering only the n-th eigenstate Sourced from [7].

where the latter expression was obtained by applying Berry's connection's (2.25) to the vector d/dt. Clearly, $g(t)$ is the shorthand for $g(\mathbf{R}(t))$, in order to have a clearer notation.

Let the elements $g \in U(1)$ be parametrized as $e^{i\eta_n(t)}$ [7], $\eta_n(t) \in \mathbb{R}$. Hence:

$$\frac{d\eta_n(t)}{dt} = -\langle n(\mathbf{R}(t))\big|\frac{d}{dt}\big|n(\mathbf{R}(t))\rangle \tag{2.51}$$

from which it can be easily obtained [7]:

$$\begin{aligned}\eta_n(T) &= i\int_0^T \langle n(\mathbf{R}(t'))\big|\frac{d}{dt'}\big|n(\mathbf{R}(t'))\rangle\, dt' \\ &= i\int_0^T \langle n(\mathbf{R})\big|\nabla_{\mathbf{R}}\big|n(\mathbf{R})\rangle\, \frac{d\mathbf{R}(t')}{dt'}dt' \\ &= i\oint_{\mathcal{C}} \mathcal{A}_n(\mathbf{R})\cdot d\mathbf{R} \\ &= \gamma_n(\mathcal{C})\end{aligned} \tag{2.52}$$

where, in the final step, we used the definition of Berry's connection after recalling that $\mathbf{R}(0) = \mathbf{R}(T) = \bar{\mathbf{R}}$; $\mathcal{C}$ denotes the closed path followed by $\mathbf{R}$ in parameter space, thus $\mathcal{C} \in C_{\bar{\mathbf{R}}}$. From (2.49) follows directly that the horizontal lifting can be written as [7]:

$$\tilde{\mathbf{R}}(T) = |n(\mathbf{R}(0))\rangle \cdot \exp\left\{-\oint_{\mathcal{C}} \mathcal{A}_n(\mathbf{R})\cdot d\mathbf{R}\right\}. \tag{2.53}$$

The latter can be compared to the definition of holonomy group (1.77), from which it is easy to understand that the exponential term belongs to it:

$$\exp\left\{-\oint_{\mathcal{C}} \mathcal{A}_n(\mathbf{R})\cdot d\mathbf{R}\right\} = e^{i\gamma_n(\mathcal{C})} \quad \in Hol_{|n(\bar{\mathbf{R}})\rangle}(\mathcal{A}_n). \tag{2.54}$$

In Fig.2.3, an explanatory image summarizes the most significative steps of our discussion.

2.2 Berry's phase in the Aharonov-Bohm effect

This section explores one of the most common examples of Berry's phase in physics: the Aharonov-Bohm effect [27].

The above-mentioned effect showed the deep physical significance of potentials, in particular electromagnetic potentials. The magnetic Aharonov-Bohm effect, for instance, proved how a particle can be affected by the vector potential $\mathbf{A}$.
Let us clarify: consider an infinitely long solenoid carrying an electric current, which generates a magnetic field confined entirely within its interior; Aharonov and Bohm found out that the wavefunction $\Psi(\mathbf{x}, t)$ of a particle with charge e moving around outside the solenoid would gain an additional phase ΔS [27]:

$$\frac{\Delta S}{\hbar} = -\frac{e}{c\hbar}\oint \mathbf{A}\cdot d\mathbf{x} \tag{2.55}$$

where the closed line integral of the vector potential is the magnetic field's flux:

$$\oint \mathbf{A}\cdot d\mathbf{x} = \Phi\,, \tag{2.56}$$

c is the light-speed and $\hbar$ the reduced Planck's constant.

We shall now reformulate this concept — following what M. V. Berry himself wrote in his 1984 paper [1] — in order to express the result while explicitly highlighting the relation with Berry's phase.

Take into account the system shown in Fig.2.4: there is a single line of magnetic flux and a box containing particles with electric charge e which is not penetrated by the flux. This implies that at every point in space, including inside the box, the magnetic field $\mathbf{B} = \nabla\times\mathbf{A}$ is zero. Therefore, it is correct to say that if the box is transported along the closed curve C depicted in the figure, it does not intersect any points where a magnetic field is present. The Hamiltonian describing such system will be a function of the kind: $\hat{H}(\hat{\mathbf{p}} - q\mathbf{A}(\hat{\mathbf{r}}), \hat{\mathbf{r}} - \mathbf{R})$ and the eigenvalue equation:

$$\hat{H}(\hat{\mathbf{p}} - q\mathbf{A}(\hat{\mathbf{r}}), \hat{\mathbf{r}} - \mathbf{R})\,|n(\mathbf{R})\rangle = E_n\,|n(\mathbf{R})\rangle\ . \tag{2.57}$$

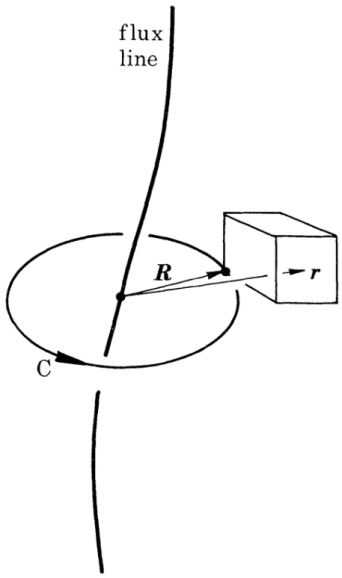

Fig. 2.4: The system assembled for the re-interpretation of the Aharonov-Bohm effect as described in the text. Sourced from [1].

Its solutions are represented by wavefunctions of the following form:

$$\langle \mathbf{r}|n(\mathbf{R}\rangle = exp\left\{\frac{ie}{\hbar}\int_{\mathbf{R}}^{\mathbf{r}} \mathbf{A}(\mathbf{r}')\cdot d\mathbf{r}'\right\}\Psi_n(\mathbf{r}-\mathbb{R}) \tag{2.58}$$

where $\Psi_n(\mathbf{r}-\mathbb{R})$ is the wavefunction of the particle at $\mathbf{r}-\mathbb{R}$ position of the box in the absence of the magnetic field [18] and the exponential factor is the Dirac phase factor[7]. It is possible to prove that, transporting[8] the box along C, the wavefunction will acquire a geometrical phase, that is Berry's phase. Let indeed calculate:

$$\begin{aligned}
&\langle n(\mathbf{R})|\nabla_{\mathbf{R}} n(\mathbf{R})\rangle = \\
&\quad = \iiint d^3\mathbf{r}\Psi_n^*(\mathbf{r}-\mathbf{R})\left\{\frac{-ie}{\hbar}A(\mathbf{R})\Psi_n(\mathbf{r}-\mathbf{R}) + \nabla_{\mathbf{R}}\Psi_n^*(\mathbf{r}-\mathbf{R})\right\} \\
&\quad = \frac{-ie}{\hbar}\mathbf{A}(\mathbf{R})
\end{aligned} \tag{2.59}$$

[7]This factor manages to keep the wavefunction $\langle \mathbf{r}|n(\mathbf{R}\rangle$ single-valued.
[8]It is not actually necessary for the transport to be adiabatic.

in order to eventually use (2.26):

$$\begin{aligned}\gamma_n(C) &= i \oint_C \frac{-ie}{\hbar}\mathbf{A}(\mathbf{R}) \cdot d\mathbf{R} \\ &= \frac{e}{\hbar}\oint_C \mathbf{A}(\mathbf{R}) \\ &= \frac{e\Phi}{\hbar}\,.\end{aligned} \tag{2.60}$$

In this way, we have been led back to the same form of equation (2.60). We note that the sign is opposite and that a $1/c$ factor is missing; these differences are not essential and they are determined by the choice of problem setup.
It is evident that this phase factor does not depend on the state n nor on C — provided that the box went around the flux line once.

As we mentioned in subsection 2.26, Berry's phase is an observable, and it can indeed be observed in the interference between particles transported around C and others kept still [1].

2.3 Berry's quantities in two-level systems: magnetic monopole and geometric interpretation

We shall now deal with a crucial example, which will be useful in order to understand the physical significance of Berry's quantities.

Consider a three-dimensional parameter space, where $\mathbf{R} = (R_1, R_2, R_3)$, where the loop $\mathcal{C}$ is located close to a degeneracy point $\mathbf{R}^*$[9]. This means that the sum in (2.40) will be dominated by the states involved in the degeneracy.

Suppose only two states, $|+\rangle$ and $|-\rangle$, involved in the degeneracy at $\mathbf{R}^*$: $E_+(\mathbf{R}^*) = E_-(\mathbf{R}^*)$ and $E_+(\mathbf{R}) > E_-(\mathbf{R})$ when $\mathbf{R} \neq \mathbf{R}^*$. Also, in a neighborhood of $\mathbf{R}^*$, the Hamiltonian $\hat{H}(\mathbf{R})$ can be expanded to first order in $(\mathbf{R} - \mathbf{R}^*)$.
To streamline the calculation and without loss of generality we can set the degeneracy at the origin $\mathbf{R} = (0, 0, 0)$ and $E_\pm(\mathbf{R}) = 0$.

The most convenient and general way to express the Hamiltonian $\hat{H}(\mathbf{R})$ of such two-level system in a three-dimensional space is as a 2x2 hermitian matrix, i. e. [1]:

$$\hat{H}(\mathbf{R}) = \frac{1}{2}\mathbf{R} \cdot \hat{\boldsymbol{\sigma}} = \frac{1}{2}\begin{bmatrix} R_3 & R_1 - iR_2 \\ R_1 + iR_2 & -R_3 \end{bmatrix} \tag{2.61}$$

[9] At this point, different states have the same eigenvalues, that is, the same energy.

where $\hat{\boldsymbol{\sigma}} = (\sigma_1, \sigma_2, \sigma_3)$ is the vector operator incorporating the three Pauli spin matrices:

$$\sigma_1 = \begin{bmatrix} 0 & 1 \\ 1 & 0 \end{bmatrix}, \quad \sigma_2 = \begin{bmatrix} 0 & -i \\ i & 0 \end{bmatrix}, \quad \sigma_3 = \begin{bmatrix} 1 & 0 \\ 0 & -1 \end{bmatrix}. \tag{2.62}$$

The eigenvalues of the Hamiltonian matrix (2.61) are:

$$E_{\pm}(\mathbf{R}) = \pm \frac{|\mathbf{R}|}{2}. \tag{2.63}$$

Due to the form in which we expressed $\hat{H}(\mathbf{R})$ (2.61), $\nabla \hat{H}$ acquires a peculiarly simply form [1]:

$$\nabla \hat{H} = \frac{1}{2} \hat{\boldsymbol{\sigma}}. \tag{2.64}$$

At this point, we can apply transformations in parameters space, rotating the axes until $\mathbf{R}$ lies in the same direction of R_3.
Knowing how Pauli matrices acts on the states $|+\rangle$ and $|-\rangle$[10]:

$$\hat{\sigma_1} |\pm\rangle = |\mp\rangle, \quad \hat{\sigma_2} |\pm\rangle = \pm i |\mp\rangle, \quad \hat{\sigma_3} |\pm\rangle = \pm |\mp\rangle \tag{2.65}$$

makes quite easy to compute $\mathcal{V}_+(\mathbf{R})$:

$$\begin{aligned} \mathcal{V}_{1+} &= \frac{\Im(\langle +|\sigma_2|-\rangle \langle -|\sigma_3|+\rangle)}{2R^2} = 0, \\ \mathcal{V}_{2+} &= \frac{\Im(\langle +|\sigma_3|-\rangle \langle -|\sigma_1|+\rangle)}{2R^2} = 0, \\ \mathcal{V}_{3+} &= \frac{\Im(\langle +|\sigma_1|-\rangle \langle -|\sigma_2|+\rangle)}{2R^2} = \frac{1}{2R^2} \end{aligned} \tag{2.66}$$

which is exactly what we expected after rotating the axes.
The result is complete as $\mathcal{V}_+(\mathbf{R}) = -\mathcal{V}_-(\mathbf{R})$.

Reinstating the initial orientation [1]:

$$\mathcal{V}_+(\mathbf{R}) = \frac{\mathbf{R}}{2R^3}. \tag{2.67}$$

The form we arrived at for the curvature $\mathcal{V}_+(\mathbf{R})$ corresponds to the form of the field generated by a monopole located at the origin [26] with a "magnetic charge" $e_M = 1/2$ [18].

[10]These states are represented in the two-dimensional state space as: $|+\rangle = \begin{bmatrix} 1 \\ 0 \end{bmatrix}$ and $|-\rangle = \begin{bmatrix} 0 \\ 1 \end{bmatrix}$

Finally, we are now equipped to compute[11] Berry's phase through (2.37):

$$\begin{aligned}\gamma_{\pm}(\mathcal{C}) &= -\iint\limits_{\Sigma(\mathcal{C})} \mathcal{V}_{\pm}(\mathbf{R}) \cdot d\mathbf{S} \\ &= \mp \iint\limits_{\Sigma(\mathcal{C})} \frac{\mathbf{R}}{2R^3} \cdot d\mathbf{S} \\ &= \mp \frac{1}{2}\Omega(\mathcal{C})\end{aligned} \tag{2.68}$$

where $\Omega(\mathcal{C})$ is the solid angle subtended by $\mathcal{C}$. Once again, with this latter, the entirely geometric nature of Berry's phase is pointed out; in such a case as the one of the two-level system, its value depends only on the solid angle $\Omega(\mathcal{C})$, which means that as long as it remains the same, $\mathcal{C}$ may assume any form.

A similar interpretation is also applicable in the case of Berry's phase for a spin-1/2 system, leading to the same result (see chapter 5.6.4, [18]).

To conclude, we shall find another remarkable result regarding the magnetic monopole, known as *Dirac quantization*. Let us consider two different surfaces Σ_1, Σ_2, both enclosed by the same loop $\mathcal{C}$ in the parameter space. Hence, since Berry's phase is an observable, the following condition should be satisfied:

$$\iint\limits_{\Sigma_1(\mathcal{C})} \mathcal{V}(\mathbf{R}) \cdot d\mathbf{S} = \iint\limits_{\Sigma_2(\mathcal{C})} \mathcal{V}(\mathbf{R}) \cdot d\mathbf{S} + 2N\pi, \quad \text{with } N = 0, \pm 1, \pm 2, ... \tag{2.69}$$

Now, defined the closed surface $\Sigma(\mathcal{C})$ as the "union" of Σ_1 and Σ_2, and given the right-hand rule as a method to consistently associate the orientation of $d\mathbf{S}$, we can get to:

$$\oiint\limits_{\Sigma(\mathcal{C})} \mathcal{V}(\mathbf{R}) \cdot d\mathbf{S} = 2N\pi. \tag{2.70}$$

Since we are currently discussing a three-dimensional problem, we can easily apply Stokes' theorem in order to obtain:

$$\oiint\limits_{\Sigma(\mathcal{C})} \mathcal{V}(\mathbf{R}) \cdot d\mathbf{S} = \oint_{\mathcal{C}} \mathcal{A}_n(\mathbf{R}) \cdot d\mathbf{R}. \tag{2.71}$$

Studying the magnetic monopole in the context of electromagnetism and gauge fields [18], we find out that (2.71) results in:

$$\frac{e}{\hbar c} 2e_M 2\pi = 2N\pi \tag{2.72}$$

[11] We can make use of spherical coordinates. Given $\theta \in [0, \pi]$ and $\phi \in [0, 2\pi]$: $d\mathbf{S} = R^2 \sin\theta d\theta d\phi \hat{\mathbf{R}}$, $\mathbf{R} = |\mathbf{R}|(\sin\theta\cos\phi, \sin\theta\sin\theta\sin\phi, \cos\theta)$, we will get: $\mathbf{R} \cdot d\mathbf{S} = |\mathbf{R}|^2 d\Omega$.

which can be re-written as:

$$e_M = \frac{\hbar C}{2e} N. \tag{2.73}$$

The latter corresponds to the condition of the already mentioned Dirac quantization: if a magnetic monopole will ever found in nature, its magnitude should be quantized as in (2.73).

2.4 Generalization: non-Abelian Berry's phase

Some months after the release of Berry's work [1], a paper by F. Wilczek and A. Zee [3] addressing a non -Abelian type of geometric phase was also published. The form of the geometric phase they found was a generalization of the one introduced by M. Berry.
This type of phase arises when the system exhibits degeneracies. In other words, in this subsection we will see what really happens when considering the degenerate case without any approximation, i. e., we will generalize and analyze more accurately the situation addressed in Subsec.2.3.

We shall now proceed following the usual path — the same we used while proving adiabatic theorem in Subsec.2.1.1 — studying the evolution of the Hamiltonian $\hat{H}(\mathbf{R})$ in parameter space; however, the n-th energy level is supposed to be N-times degenerate. It is possible to set the degeneracy level at zero: $E_n = 0$ through a simple renormalization (analogous to (2.46)). Moreover, the n-th level will be assumed to be separated from the other energy levels.

Suppose now that the parameters vary slowly enough to allow the use of the adiabatic limit from $\mathbf{R}(0)$ to $\mathbf{R}(T)$, with $\mathbf{R}(0) = \mathbf{R}(T)$. Hence, the time-dependent Schrödinger equation (2.2) will map the solutions of:

$$\hat{H}(\mathbf{R}(0)) \left| n_a(\mathbf{R}(0)) \right\rangle = 0 \tag{2.74}$$

onto solutions of:

$$\hat{H}(\mathbf{R}(T)) \left| n_a(\mathbf{R}(T)) \right\rangle = 0. \tag{2.75}$$

We used $|n_a(\mathbf{R}(t))\rangle$ to denote the N eigenstates making up a basis for the degenerate eigenspace; the subscript $a = 1, ..., N$ labels the degenerate states. Nonetheless, when $N \neq 1$, this map is not trivial. Thus, a general solution with initial condition $|\psi_a(\mathbf{R}(0)\rangle = |n_a(\mathbf{R}(0)\rangle$ is written as [3]:

$$\left| \psi_a(\mathbf{R}(t)) \right\rangle = U_{ab}(\mathbf{R}(t)) \left| n_b(\mathbf{R}(t)) \right\rangle . \tag{2.76}$$

where $U(\mathbf{R}(t))$ is some unitary operator.
To find the right form of the operator, we can require the normalization of the $|\psi_a(\mathbf{R}(t)\rangle$

state to be preserved, namely:

$$\langle \psi_b | \dot{\psi}_a \rangle = \langle \psi_b | \dot{U}_{ac} n_c \rangle + \langle \psi_b | U_{ac} \dot{n}_c \rangle = 0 \tag{2.77}$$

where $|\psi(\mathbf{R}(t)\rangle = |\psi\rangle \, , U = U(\mathbf{R}(t)), |n(\mathbf{R}(t))\rangle = |n\rangle$ for clearness's sake.
Since this has to always hold true, we get to [3]:

$$[U^{-1}(\mathbf{R}(t))\dot{U}(\mathbf{R}(t))]_{ba} = \langle n_b(\mathbf{R}(t)) | \dot{n}_a(\mathbf{R}(t)) \rangle \equiv \mathcal{A}_{n,ab}(\mathbf{R}(t)) \tag{2.78}$$

We thus defined the components of an anti-Hermitian matrix $\mathcal{A}_n$, referred to as *Wilczek-Zee matrix*. This is the generalization of the connection one-form we dealt with when studying the Abelian case (2.25).
Its specific form clearly depends on the choice of the basis. If we had chosen a different one, we would have obtained a different state, related to the first one by:

$$|\psi'(\mathbf{R}(t))\rangle = T(\mathbf{R}(t)) \, |\psi(\mathbf{R}(t))\rangle \, . \tag{2.79}$$

Hence, the connection matrix transforms as:

$$\mathcal{A}_n(\mathbf{R}(t)) = \dot{T} T^{-1} + T \mathcal{A}_n T^{-1}. \tag{2.80}$$

Note the similarity in form of the latter equation with the general transformation equation for connection one-forms (1.70).

From (2.78), the expression for $U(\mathbf{R}(t))$, that we shall denote with $\Gamma(\mathbf{R}(t))$ from now on, is:

$$\begin{aligned} \Gamma(\mathbf{R}(t)) &= \mathcal{P} \exp \left\{ \int_0^T \mathcal{A}_n(\mathbf{R}(t)) \cdot dt \right\} \\ &= \mathcal{P} \exp \left\{ \int_{\mathbf{R}(0)}^{\mathbf{R}(T)} \mathcal{A}_n(\mathbf{R}) \cdot d\mathbf{R} \right\} \end{aligned} \tag{2.81}$$

where $\mathcal{P}$ is the path-ordering operator.
If we then denote the loop completed by the Hamiltonian $\hat{H}(\mathbf{R}(t))$ in the parameter space (recall that we previously mentioned $\mathbf{R}(0) = \mathbf{R}(T)$) as $\mathcal{C}$, we can express Γ in a form that makes its purely geometric dependence on the loop explicit:

$$\begin{aligned} \Gamma(\mathcal{C}) &= \mathcal{P} \exp \left\{ \oint_{\mathcal{C}} \mathcal{A}_n(\mathbf{R}) \cdot d\mathbf{R} \right\} \\ &= \Gamma(\mathcal{C}). \end{aligned} \tag{2.82}$$

This quantity is the generalization of the Berry's phase, i. e., the non-Abelian version of it acting in the degenerate subspace. It is also referred to as *Wilson loop* [3].

It is possible to associate non-Abelian Berry's curvature, a second-rank tensor, which reads as [7]:

$$\mathcal{V}_{n,\mu\nu}(\mathbf{R}) = \frac{\partial}{\partial R^{\mu}}\mathcal{A}_{n,\nu}(\mathbf{R}) - \frac{\partial}{\partial R^{\nu}}\mathcal{A}_{n,\mu}(\mathbf{R}) + [\mathcal{A}_{n,\mu}, \mathcal{A}_{n,\nu}]. \tag{2.83}$$

As was done in the Abelian case, we can now point out the geometric interpretation of the problem on a principal fiber bundle [28].
Again, we can think of the parameter space as the base space B, while the fibers will each be a copy of the structure group, which in this case is represented by $U(N)$:

$$\pi^{-1}(R) \cong U(N). \tag{2.84}$$

Indeed, this time the evolution of the quantum states is not embodied by a "simple" phase factor, but it involves unitary matrices. Note that, how we expected, $U(N)$ is not Abelian, since the binary operation, i.e., matrices multiplication, is not commutative. We can see that, in (2.83), the commutator term does not vanish — as it happens in the Abelian case instead, see (2.42).

Eventually, assigning $\bar{\mathbf{R}} = \mathbf{R}(0) = \mathbf{R}(\mathbf{T})$, the Wilczek-Zee matrix defines the element of the holonomy group $Hol_{|n(\bar{\mathbf{R}})\rangle}(\mathcal{A}_n) \subset U(N)$.

3 Applications to quantum technologies

Quantum technology is a form of computation through which we are- at least, potentially- able to exploit purely quantum properties (such as *superposition*, *entanglement*) of physical systems. This led to a revolutionary approach to information theory and computation.

Nevertheless, the main problem is the vulnerability of quantum systems and, thus, of the quantum information we would like to handle. This very real problem played a significant role in the initiation of a general effort in finding alternatives and solution that could make up for it.

One of the possible options is the one of *topological quantum computation*, whose primary strength lies in its potential of providing highly decoherence-tolerant devices, whose robustness is intrinsically rooted in the hardware.

Through this chapter, we will introduce quantum computation and its fundamental concepts, then we will analyze its limits (decoherence, above all). Finally, an introductory address of topological quantum computation will be delivered.

3.1 A brief introduction to quantum computation

In this section we are introducing the principal concepts of quantum computation, such as qubits, quantum gates, errors and cecoherence. Establishing these ideas is necessary to effectively approach the next two sections.

3.1.1 Qubits and the Bloch sphere

The core concept of quantum computation is the **qubit**, which is shorthand for "quantum bit"; indeed, a qubit *is* the quantum version of a classical bit, capable of storing *quantum information*.

A qubit can be thought of as a mathematical object [29] with quantum properties. As a classical bit has two possible states, 0 or 1, also a qubit can be in a $|0\rangle$ or $|1\rangle$ state. However, the quantum nature of qubits allows them to be in a *superposition*, namely a linear combination, of the two "computational basis states". That is, an arbitrary state of a qubit can be written as:

$$|\psi\rangle = \alpha\,|0\rangle + \beta\,|1\rangle \quad \text{with } \alpha, \beta \in \mathbb{C}. \tag{3.1}$$

Now, physically measuring a qubit actually means *destroying* its state, collapsing it to either $|0\rangle$ or $|1\rangle$, the first one with a $|\alpha|^2$ probability, the second one with a $|\beta|^2$ probability. This implies: $|\alpha|^2 + |\beta|^2 = 1$.
It is logical to describe the qubit as a two-dimensional unit vector lying in a two-dimensional complex vector space, say a *Hilbert space*[1], where $|0\rangle$ and $|1\rangle$ act as an orthonormal basis. It is conventional the correspondence:

$$|0\rangle = \begin{pmatrix} 1 \\ 0 \end{pmatrix}, \quad |1\rangle = \begin{pmatrix} 0 \\ 1 \end{pmatrix} \tag{3.2}$$

which makes the arbitrary state appear as:

$$|\psi\rangle = \begin{pmatrix} \alpha \\ \beta \end{pmatrix}. \tag{3.3}$$

It is possible to exploit the fact that $|\alpha|^2 + |\beta|^2 = 1$ always holds true in such a way that, given $\gamma, \theta, \varphi \in \mathbb{R}$, we can write an arbitrary state as [29]:

$$\begin{aligned} |\psi\rangle &= e^{i\gamma} \left(\cos\frac{\theta}{2} |0\rangle + e^{i\varphi} \sin\frac{\theta}{2} |1\rangle \right) \\ &= \cos\frac{\theta}{2} |0\rangle + e^{i\varphi} \sin\frac{\theta}{2} |1\rangle \end{aligned} \tag{3.4}$$

with $\gamma \in [0, 2\pi), \theta \in [0, \pi]$ and $\varphi \in [0, 2\pi)$. In (3.4), we were able to dispose of the $e^{i\gamma}$ thanks to the fact that the global phase does not affect the observable quantity — as we have already stressed several times. Equations (3.4) naturally suggest an isomorphism between the unit S^2 sphere and the states of a single qubit. The sphere is referred to as **Bloch sphere**. Its surface's points — and thus, the qubit's (pure) states — are defined by the two angles θ and φ (see Fig.3.1).

Remark. Recall the construction of the Hopf bundle we studied in 1.4.5. Given the north pole as the stereographic projection pole, we can recognize in the base space S^2 the Bloch sphere. Then, the single qubit Hilbert space is the unit three-sphere S^3 in $\mathbb{C}^2$, that is, the Hopf bundle. Thus, each circle S^1 allows to identify quantum states including the global phase shifts.

We shall now study the case of a multiple-qubits system.
Suppose we have two qubits; these will be represented by complex vectors in a four-dimensional complex vector space. As before, each qubit could be in a $|0\rangle$ or $|1\rangle$ state,

[1] A Hilbert space $\mathcal{H}$ is a vector space equipped with an inner product, where quantum states are rapresented as vectors

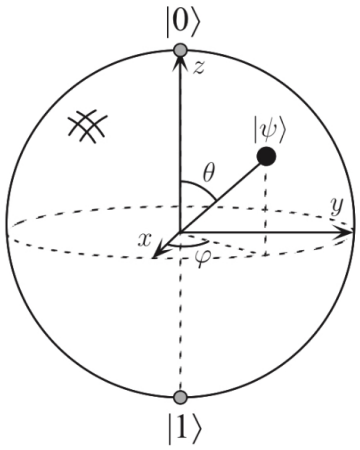

Fig. 3.1: Representation of the Bloch sphere. To each point on its surface, a quantum state is associated. Sourced from [29].

or in a superposition of those. This means that a general expression of the whole system will be[2]:

$$|\psi\rangle = \alpha_{00}\,|00\rangle + \alpha_{01}\,|01\rangle + \alpha_{10}\,|10\rangle + \alpha_{11}\,|11\rangle\,. \tag{3.5}$$

This also implies that the computational basis here is made up of: $|00\rangle + |01\rangle + |10\rangle + |11\rangle$ and the physical meaning of the coefficients stays the same: a $|ij\rangle$ measure occurs with probability $|\alpha_{ij}|^2$. Clearly, the normalization condition for the coefficients $\sum_{i,j=0} |\alpha_{ij}|^2 = 1$ still holds [29].
We could of course decide to measure a subset of the qubits in the system. Since we are considering a two-qubits system, let us see what happens when measuring the first qubit: we would end up with measuring it in the $|0\rangle$ state with $(|\alpha_{00}|^2 + |\alpha_{01}|^2)$ probability or in the $|1\rangle$ state with $(|\alpha_{10}|^2 + |\alpha_{11}|^2)$ probability. If, for instance, the result of the measure is $|0\rangle$, the system will then find itself in the following modified state:

$$|\psi'\rangle = \frac{\alpha_{00}\,|00\rangle + \alpha_{01}\,|01\rangle}{\sqrt{|\alpha_0 0|^2 + |\alpha_0 1|^2}} \tag{3.6}$$

where the factor in the denominator is necessary in order to re-normalize the finale state.

In multiple-qubits system, a very peculiar event can occur: *entanglement*.
Let us consider the following state:

$$|\Phi^+\rangle = \frac{1}{\sqrt{2}}\big(\,|00\rangle + |11\rangle\,\big). \tag{3.7}$$

[2]The $|ij\rangle$ notation $|ij\rangle$ stands for: "the first qubit is in the state $|i\rangle$, the second one in the state $|j\rangle$ ".

Measuring the first qubit would give as a result: $|0\rangle$, with 1/2 probability and $|1\rangle$, with 1/2 probability. The state of the system after the measurement will be, respectively, the following: $|00\rangle$ or $|11\rangle$. This is what entanglement consists of: by measuring one of the two qubits, we can determine the state of both. In this case, we know *a priori* that the two qubits will share the same state.
For completeness, here is the most commonly used computational basis for a two entangled qubits system, called *Bell's states*:

$$\begin{aligned} |\Phi^+\rangle &= \frac{1}{\sqrt{2}}\big(\,|00\rangle + |11\rangle\,\big), \quad |\Phi^-\rangle = \frac{1}{\sqrt{2}}\big(\,|00\rangle - |11\rangle\,\big), \\ |\Psi^+\rangle &= \frac{1}{\sqrt{2}}\big(\,|01\rangle + |10\rangle\,\big), \quad |\Psi^-\rangle = \frac{1}{\sqrt{2}}\big(\,|01\rangle - |10\rangle\,\big). \end{aligned} \tag{3.8}$$

An entangled state *cannot* be separated, that is: $|\psi_{12,entangled}\rangle \neq |\psi_1\rangle \otimes |\psi_2\rangle$.

Remark. It is indeed possible to provide a geometric representation of a two-qubits system, similar to the one-qubit case, using the S^7 Hopf bundle in $\mathbb{C}^4$. We limit ourselves to stating that the conceptually and mathematically complex geometry underlying this framework also allows for a geometric interpretation of entangled states.

Experimentally, qubits can be obtained with physical quantum systems able to represent the $|0\rangle$ and $|1\rangle$ states. For instances, one can use spins (up $|\uparrow\rangle$ and down $|\downarrow\rangle$), polarized photons (horizontal $|\leftrightarrow\rangle$ and vertical $|\updownarrow\rangle$ polarization) or any state that can provide a two-level configuration.

3.1.2 Quantum gates

In order to actually *do* quantum computation, we need quantum gates, which are the "quantum counterpart" of classical logic gates. Essentially, at a mathematical level, quantum gates are linear, unitary[3] operators acting on vectors representing the state of a qubit. We can thus think of them as elements of $U(n)$, where n is the dimension of the vector space where the operator acts.

It is worth emphasizing that, unlike classical gates, quantum gates are always reversible- which is a consequence of the unitarity request; in addition, another fundamental difference is the fact that qubits *cannot* be cloned, as there does not exist any unitary transformation capable of performing such an operation (this is known as the *No-cloning theorem*, see chapter 12.1.1, [29]).

For a single qubit, quantum gates are 2x2 unitary matrices $\in U(2)$. We list below the most important and commonly used ones.

[3] An operator U is said unitary if $U^\dagger U = \mathbb{I}$. Unitarity is necessary to preserve probability.

- ***NOT* gate:**

$$X \equiv \begin{pmatrix} 0 & 1 \\ 1 & 0 \end{pmatrix} \tag{3.9}$$

swaps the states $|0\rangle$ and $|1\rangle$:

$$X|0\rangle = |1\rangle\,, \quad X|1\rangle = |0\rangle\,. \tag{3.10}$$

- ***Z* gate:**

$$Z \equiv \begin{pmatrix} 1 & 0 \\ 0 & -1 \end{pmatrix} \tag{3.11}$$

applies a phase shift of π to the state $|1\rangle$, leaving $|0\rangle$ unchanged:

$$Z|0\rangle = |0\rangle\,, \quad Z|1\rangle = -|1\rangle\,. \tag{3.12}$$

- ***Hadamard* gate:**

$$H \equiv \frac{1}{\sqrt{2}} \begin{pmatrix} 1 & 1 \\ 1 & -1 \end{pmatrix} \tag{3.13}$$

transforms the basis states into superpositions:

$$H|0\rangle = \frac{|0\rangle + |1\rangle}{\sqrt{2}} \equiv |+\rangle\,, \quad H|1\rangle = \frac{|0\rangle - |1\rangle}{\sqrt{2}} \equiv |-\rangle \tag{3.14}$$

where $|+\rangle\,, |-\rangle$ represent another possible choice for a computational basis.

There exists an infinite number of quantum gates (acting on single or multiple qubits), since any unitary transformation corresponds to one.

Remark. Reversibility implies that the number of qubits entering a quantum gate is equal to the number of qubits exiting it.

The prototype for a two-qubits gate is the $CNOT$ gate, which stands for "controlled-not" gate. Given two qubits, initially at $|A\rangle$ and $|B\rangle$, a NOT transformation (3.9) is applied to the second qubit iff the the first is in the 1 state when measured. The action of a $CNOT$ gate is shown through a diagram in Fig.3.2, where $|B \oplus A\rangle$[4] effectively embodies it. For instance, given an initial state $|10\rangle$, after the action of a $CNOT$ gate it will become a $|11\rangle$ state.

$CNOT$ gate is also representable through a 4x4 matrix $U_{CN} \in U(4)$:

[4]The $\oplus$ symbol stays this time for "modulo two operation".

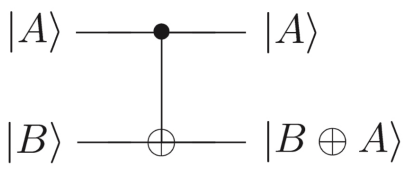

Fig. 3.2: Diagrammatic representation of the quantum CNOT gate. Sourced from [29].

$$U_{CN} \equiv \begin{pmatrix} 1 & 0 & 0 & 0 \\ 0 & 1 & 0 & 0 \\ 0 & 0 & 0 & 1 \\ 0 & 0 & 1 & 0 \end{pmatrix} = \begin{pmatrix} \mathbb{I} & 0 \\ 0 & X \end{pmatrix} \tag{3.15}$$

where we highlighted the identity matrix $\mathbb{I}$ and the NOT matrix X.
A similar type of quantum gate can be analogously implemented as a controlled-Z gate, CZ, replacing the "X" block in (3.15) with a "Z" block:

$$U_{CZ} = \begin{pmatrix} \mathbb{I} & 0 \\ 0 & Z \end{pmatrix}. \tag{3.16}$$

It has actually been showed that single-qubit gates together with $CNOT$ gate constitute a *universal* set for quantum computing, that is, finite combinations of $CNOT$ gates and rotations of single-qubit can approximate with arbitrary precision any other two-qubit transformation [29].

3.1.3 Quantum noise and quantum states decoherence

In order to build quantum computers, once a physical system capable of acting as qubits is chosen, the next step is to assemble quantum gates into a functional quantum circuit. Quantum circuits differ significantly from classical ones; for instance, they are inherently non-cyclic, and their "wires" often represent the flow of time or particles.

Another important aspect to consider when dealing with quantum computers is their vulnerability to external factors, making them challenging to operate.
What we have said so far runs smoothly as far as we manage to keep the system closed. However, perfectly closed *real* systems do not exists and thus, most of the time, our physical system — within which quantum information is encoded — inevitably interacts with the surrounding environment.

This interaction introduces what is commonly referred to as *noise*, which threatens the *quantumness* of the entire process [30]. Noise jeopardizes the system, potentially reducing the quantum computer to a classical one by invalidating the quantum principles we rely on to manipulate quantum information.

Indeed, interactions destroy the quantum state, causing **decoherence**, that is, the relative phase between components of a quantum superposition is disrupted. The *pure* quantum state (such as the one shown in (3.1)) transitions into a *mixed* state, entangled to the environment, neither fully quantum anymore, nor entirely classical yet[5].

Moreover, measurement itself introduces decoherence and acts as a form of noise, making it seem impossible to address these problems.

Theory of **quantum error correction** aims to mitigate the effects of decoherence. It provides methods to detect and correct errors, without directly measuring the quantum system.
This is often achieved by introducing additional qubits, known as *ancilla* qubits, and encoding logical qubits $|0\rangle_L = |000\rangle$ and $|1\rangle_L = |111\rangle$ into a group of physical qubits (as introduced in Subsec.3.1.1). Indirect measurements, called *syndromes*, allow error detection without collapsing the quantum state.

Furthermore, systematic errors — hardware-level imperfections — and the finite precision of quantum gates introduce additional challenges. Even small inaccuracies in gate implementation can lead to failures, further complicating the process.

In summary, quantum computers are subject to a wide range of factors that could compromise their efficiency and accuracy, making them both challenging to construct and operate.

3.2 Topological quantum computation

Global properties of manifolds that are generally unaffected by local deformations can be studied through *topology*.
In this section, after introducing some useful definitions in order to deal with fundamental topology concepts, we will provide an idea of how these global properties of manifolds could, at least theoretically, be exploited at material level and used to construct decoherence-free quantum computers.

We shall point out that idea of topological quantum computation was firstly addressed by the physicist A. Yu. Kitaev [4], [28].

[5]These concepts could be explored using the elegant mathematical formalism of density matrices. However, this discussion lies beyond our scope. For further reading, see, for instance, [29].

3.2.1 Topological framework: some definitions

Here, a series of additional mathematical definitions will be proposed, aimed at supporting the understanding of the next section.

Given a space X and a family $\mathcal{T}$ of subsets of X, $\mathcal{T}_i \subset X$, these are said to be **open sets** and the pair $(X, \mathcal{T})$ is called **topological space** if:

- the empty set $\varnothing$ and the entire set X are included:

$$\varnothing, X \in \mathcal{T};$$

- an arbitrary union of sets $\mathcal{T}_i \in \mathcal{T}$ is open:

$$\bigcup_i \mathcal{T}_j \in \mathcal{T};$$

- a finite intersection of sets $\mathcal{T}_i \in \mathcal{T}$ is open:

$$\bigcap_{j=1,\dots,N} \mathcal{T}_j \in \mathcal{T}.$$

X is called **underlying space** while $\mathcal{T}$ is called **topology**.

The **quotient space** $X/\sim$ is defined as the set of equivalence classes of X with respect to the equivalent relation $\sim$, that is:

$$X/\sim = \{[x] \mid x \in X\}, \tag{3.17}$$

where $[x]$ is the equivalence class of x, i.e., the set of all points $y \in X$ such that $x \sim y$.

In a topological space, it is possible to define a **path**. It can heuristically be understood as a specific parametrization of a curve (which we already characterized in Sec.1.1) with a direction and endpoints. Formally, it is a continuous map $\lambda : [0,1] \subset \mathbb{R} \to X$, where X is the topological space[6]. The *endpoints* of the path are $\lambda(0)$, called **starting point**, and $\lambda(1)$, called **ending point**. These define a *direction* for the path.
Whenever the two endpoints coincide $\lambda(0) = \lambda(1) = x$ the path is referred to as a **loop** at x.

Now, two paths on the same space can be compared, In particular, there can exists a peculiar relation between the two, namely a *homotopy* relation.
Consider two paths $\lambda_1, \lambda_2 : [0,1] \to X$ on the same topological space X, with fixed

[6]It would have been more precise to say "a space on which we can define a topology".

sharing endpoints, that is: $\lambda_1(0) = \lambda_2(0) = x_0$ and $\lambda_1(1) = \lambda_2(1) = x_1$. An **homotopy** between λ_1 and λ_2 is a continuous map $F : [0,1] \times [0,1] \to X$ such that:

$$F(s,0) = \lambda_1(s), \quad F(s,1) = \lambda_2(s) \quad \forall s \in [0,1], \tag{3.18}$$

$$F(0,t) = x_0, \quad F(1,t) = x_1 \quad \forall t \in [0,1]. \tag{3.19}$$

If such a map does exists, then λ_1 and λ_2 are said to be **equivalent** or **homotopic** paths, in symbols: $\lambda_1 \sim \lambda_2$. This latter indeed expresses an equivalence relation.

This definition can of course be naturally extended to loops as well [7].

As an example, consider a loop $\lambda : [0,1] \to \mathbb{R}^2$ based at a point $x_0 \in \mathbb{R}^2$. The loop can be continuously shrunk to the point x_0 using the homotopy:

$$F(t,s) = (1-s)\lambda(t) + sx_0,$$

where t parametrizes the loop, and s represents the deformation parameter. For $s = 0$, $F(t,0) = \lambda(t)$, and for $s = 1$, $F(t,1) = x_0$.
This demonstrates that any loop in $\mathbb{R}^2$ is homotopic to the constant loop at x_0, and thus any two loop in $\mathbb{R}^2$ are homotopic.

From the concept of homotopy derives the concept of **fundamental group** $\pi_1(X, xo)$. It is the set of all homotopy classes $[\lambda]$ of loops λ at x_0 equipped with a group structure (see Subsec.1.4.2) under the binary operation $[\lambda] \cdot [\gamma] \equiv [\lambda * \gamma]$, $[\lambda], [\gamma], [\lambda * \gamma] \in \pi_1(X, x_0)$ [31], called *concatenation map* and described as:

$$(\lambda * \gamma)(t) = \begin{cases} \lambda(2t), & \text{se } t \in [0, 1/2], \\ \gamma(2t-1), & \text{se } t \in [1/2, 1]. \end{cases} \tag{3.20}$$

Essentially, the fundamental group consists of all loops that can be continuously deformed into one another, corresponding to the concept of homotopy.

Recalling the example above, the fundamental group of $\mathbb{R}^2$ at a fixed point $x_0 \in \mathbb{R}^2$ is: $\pi_1(\mathbb{R}^2, x_0) = \{[x_0]\} = \{e\}$, namely, the unit element. Clearly, the presence of a "hole" or any other type of obstacle would change this situation, and we would no longer be able to say that any loop is equivalent to every other loop.

3.2.2 Abelian and non-Abelian Anyons

Given an N point-like indistinguishable particles quantum system, we can study the case when two particles are exchanged. Essentially, the wavefunction of the system $\psi(1, 2, ..., N)$ acquires a phase factor $e^{i\Phi}$, with $\Phi = 0, \pi$, when two particles are exchanged, i. e.:

$$\psi(1, 2, ..., i, ..., j, ..., N) = e^{i\Phi}\psi(1, 2, ..., j, ..., i, ..., N) \tag{3.21}$$

In three dimensions, the wavefunction can stay the same $e^{i0} = 1$ or change sign $e^{i\pi} = -1$. In two dimensions, instead, Φ can take an arbitrary value $\in [0, \pi]$, or, in some cases, the exponential $e^{i\Phi}$ can be replaced by a unitary matrix.

This can be better understood by looking at topological properties of the paths in space-time that describe the exchange of two particles (see Fig.3.3). In particular, we shall consider their configuration space. As argued in [23], the configuration space of N identical particles, each moving in $\mathbb{R}^d$, with $d \geq 2$, is defined by the following topological space:

$$Q = (\mathbb{R}^{Nd} - \Delta)/P_N \tag{3.22}$$

where $\mathbb{R}^{Nd} = \mathbb{R}^d \times \mathbb{R}^d \times .... \times \mathbb{R}^d$, N times, is a product space, Δ is the *diagonal* of $\mathbb{R}^{Nd}$ defined by:

$$\Delta = \{\mathbf{x}_1....\mathbf{x}_N; \mathbf{x}_i \in \mathbb{R}^d \mid \mathbf{x}_i = \mathbf{x}_j \text{ for at least a pair } (i,j), i \neq j\} \tag{3.23}$$

representing the forbidden configurations where the two particles coincide. Finally, the term $/P_N$ implies we are considering the quotient by the action of P_N, which is the so-called permutation group.

Let us say something about the latter.
The **permutation group** P_N is a discrete group consisting of all possible permutations (which are mappings from a set to itself) of the N elements of a set. The group counts thus $N!$ elements, generated by $N-1$ transpositions. Transpositions $\sigma_i \in P_N$ satisfy:

$$\sigma_i \sigma_j = \sigma_j \sigma_i, \quad |i-j| \geq 2 \tag{3.24}$$

$$\sigma_i \sigma_{i+1} \sigma_i = \sigma_{i+1} \sigma_i \sigma_{i+1} \tag{3.25}$$

$$(\sigma_i)^2 = e \tag{3.26}$$

i. e., the permutation group is Abelian, the order in which permutation are applied does not count and permutations are idempotent.

Another important group, which is useful when dealing with indistinguishable particles in two dimensions ($d = 2$), is the **braid group** B_N. This infinite and discrete group is a generalization of the permutation group. Its action involves the braiding of N *strands*[7]: the braiding τ_i crosses strand i over strand $i+1$. Moreover, this group is, in general, non-Abelian, i. e., $\tau_i \tau_j \neq \tau_j \tau_i$ and — most importantly — its elements are not idempotent, that is, $(\tau_i)^2 \neq e$ (see 3.6).

We shall now state a theorem which will useful in our upcoming discussion [23].

[7] *Strands* have to be intended as trajectories of particles in space-time.

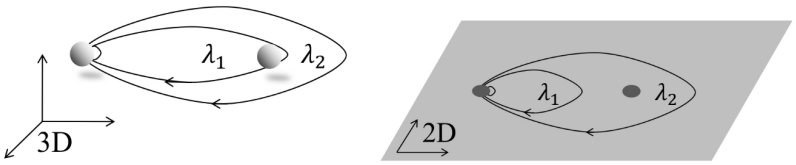

Fig. 3.3: A visual representation of the exchange of two particles is shown, in the three-dimensional case (left) and the two-dimensional one (right). Sourced from [5].

Theorem. *Given a topological space Q defined as in* (3.22)*, we can distinguish two cases:*

$$\begin{aligned} \pi_1(Q) &= P_N \quad \textit{for } d \geq 3, \\ \pi_1(Q) &= B_N \quad \textit{for } d = 2. \end{aligned} \tag{3.27}$$

In three dimensions ($d = 3$), two loops λ_1, λ_2 swapping two particles are topologically equivalent $\lambda_1 \sim \lambda_2$, that is, they belong to the same homotopy class. Indeed, we can see this process as the action of the permutation group P_2, in particular we can think of a loop as the consecutive application of σ_i and σ_i^{-1}. The fact that $(\sigma_i)^2 = e$ coincides with the fact that any loop λ in $\mathbb{R}^3$ can homotopically be deformed into another one, essentially $\lambda \sim e$.
In terms of evolution of the system, it must be such that:

$$|\psi(\lambda_2)\rangle = S^2 \, |\psi(0)\rangle \,, \quad \text{with } S^2 = 1 \tag{3.28}$$

where the ket in the left-hand side represents the final state of the system, $|\psi(0)\rangle$ is the initial state, and S^2 is the *exchange operator*[8] applied two times [5]. The condition on it leads to: $S = \pm 1$, as a confirmation of what we have stated above.
Should this be the case, the order and the orientation of the exchanges does not count and thus the statistics can be described by the permutation group.

When $\hat{S} = 1$ and the wavefunction (3.21) stays the same, the particles that made up the system are referred to as *bosons*, otherwise, when $\hat{S} = -1$ and the wavefunction switches sign, they are called *fermions*[9].

On the other hand, in two dimensions ($d = 2$), the situation is far different; what we have said for three dimensions is only possible due to rotations in third dimension. Indeed, for elements of the braid group B_2, $(\tau_i)^2 \neq e$. The structure of the configuration space does not allow the two loops λ_1 and λ_2 to be topologically equivalent in this case. Hence,

[8]The *exchange operator* is an operator that, applied to the initial state of the quantum system, gives the state of the system after the exchange of two particles.

[9]The names were chosen after the scientists who studied the associate statistics, that is S. Bose and E. Fermi.

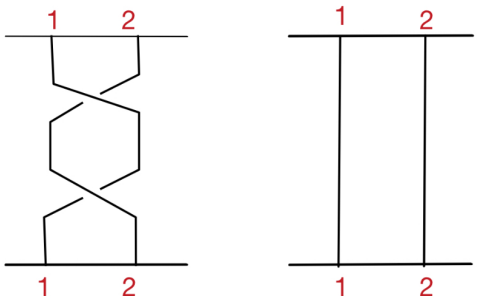

Fig. 3.4: These can be seen as example of permutations as well as braidings. If we consider the permutation group, these two elements are exactly the same (property (3.25)*), whereas, as elements of the braid group, these are different. Taken from [32].*

the constraint $S^2 = 1$ does not held anymore, and $\hat{S}$ can be represented by a generic complex phase or a unitary matrix.

At this point, peculiar particles might arise, named **anyons**[10]. In particular, when the final state of the system is obtained through a unitary matrix, we talk about **non-Abelian anyons**. The exotic behaviour of such particles leads to a type of statistics called *fractional* statistics.

Physically, they manifest as *quasiparticles*, representing collective states of the elementary excitations [5], characterized by properties that arise from the system as a whole and whose quantum evolutions are strictly related to topology in the configuration space.

3.2.3 Topological quantum computation

The idea behind topological quantum computation is to exploit topological properties of non-Abelian anyons to develop a revolutionary type of quantum computer that is significantly more resistant to decoherence compared to "ordinary" quantum computers.

This subsection is based on the analysis provided in [5].

The first obstacle is the fact that no genuine two-dimensional system exists, meaning we have to constrain systems in two-dimensions in order to *probably* observe anyonic behaviors in the materials. Indeed, two-dimensions do not guarantee the existence of anyons.

Isolated sheets of graphene, two-dimensional optical lattices of cold atoms and electrons

[10]The name *anyons* resembles "fermi*ons*, bos*ons*", but the "*any-*" prefix stand for "any direction", in the sense that Φ in $e^{i\Phi}$ can be "any" ($\in [0, \pi]$).

confined by strong magnetic fields, such as Quantum Hall Effect, are examples of real physical system constrained in two-dimensions.

Let us now give an useful definition; a **topological state** of matter is a phase of matter which is characterized by global topological properties — rather than local symmetries, which are instead typically used to classify conventional phases.

Now, all topological states that support the potential existence of anyons are insulators, which implies a strong separation Δ between the ground state and the rest of the energy states of the system.

The introduction of non-Abelian quasiparticles causes low-energy states to acquire a certain level of degeneracy, which depends on the type of anyons. This originates a decoherence-free degenerate subspace — which can be described as a manifold — that we can exploit to encode quantum information. Indeed, this protection, which is the very reason for topological quantum computation, derives from both the energy gap and the fact that the degenerate subspace is a collective non-local property of non-Abelian anyons; the first one makes unlikely any spontaneous excitations which could interact with already present anyons. At the same time, it is reasonable to think that any perturbation in the system would act as a local displacement of the anyons, which thus do not affect global properties.

The evolutions of quantum states in the protected degenerate subspace are adiabatic[11] transports of anyons on the manifold, evolving through a non-Abelian Berry's phase (see Subsec.2.4), which shows indeed a topological nature, i.e., independent from local geometry. If the dimension of the subspace is N, then, the evolution of the system's state $|\Psi_a(z_1, z_2, ..., z_n)\rangle$ depending on anyon coordinates z_j is given by:

$$|\Psi_a(z_1, z_2, ..., z_n)\rangle \mapsto \sum_{b=1}^{N} \Gamma_{ab}(\lambda) \, |\Psi_a(z_1, z_2, ..., z_n)\rangle \quad \text{with } a = 1, 2, ..., N \tag{3.29}$$

where λ denotes a cyclic path in z_j. The expression of $\Gamma(\lambda)$ is analogous to (2.82):

$$\Gamma(\lambda) = \mathcal{P} \exp\left\{ \oint_{\lambda} \mathcal{A}(\mathbf{z}) \cdot d\mathbf{z} \right\} \tag{3.30}$$

where the components $(\mathcal{A}^j)_{ba}$ of the connection $\mathcal{A}$ appear as:

$$(\mathcal{A}^j)_{ba} = \langle \Psi_b(z_1, z_2, ..., z_n)| \, \frac{\partial}{\partial z_j} \, |\Psi_a(z_1, z_2, ..., z_n)\rangle \, . \tag{3.31}$$

Hence, as mentioned, we understand that the non-Abelian Berry's phase in the context of non-Abelian anyons is strictly related to the topological properties of the system [5].

[11] In this case, "adiabatically" means "slowly compared to the energy gap Δ.

Fusion channels and braidings

We will now introduce the anyonic processes that will enable us to do quantum computation with anyons. We will refer to this theoretical model as *anyon model*.
Our discussion is based on some assumptions: anyons can be created/annihilated in pairwise fashion, they can be *fused* in order to originate other types of anyons and can be exchanged adiabatically.

The anyon model can be thought as spanned by a certain number of particles:

$$M = \{1, a, b...\} \tag{3.32}$$

where $1, a, b...$ are sort of a "topological charge" carried by each anyon; 1 stands for "vacuum's topological charge". Since these are charge, they should be conserved. Topological conservation rules are known as *fusion rules*:

$$a \times b = \sum_{c \in M} N_{ab}^{c} c. \tag{3.33}$$

The *fusion coefficients* N_{ab}^{c} are non-negative integers (most of the time, $N_{ab}^{c} = 0, 1$) which weight the possible outcomes of the fusion between a and b. If only one coefficient N_{ab}^{c} is different from zero, then the model is Abelian. On the contrary, when different coefficients are different form zero, the model is non-Abelian.
These non-Abelian anyons' fusion channel degrees of freedom create a space spanned by the possible fusion outcomes. Given, for instance, $a \times b = c + d$, the orthonormal basis for such a space:

$$\langle ab; c | ab; d \rangle = \delta_{cd} \tag{3.34}$$

where δ_{cd} is the Kronecker delta function. Whenever there are N outcomes from the fusion of two anyons, the system will acquire an N-fold degeneracy spanned by the already mentioned basis, called the *fusion space*. The latter coincides exactly with the protected degenerate subspace we introduced above.

However, two states obtained with a different fusion outcome are defined in different topological charge sectors, thus we cannot perform superposition with them.
A possible way to overcome this problem is using more than two anyons in order to fuse them in different ways but ending up with the same type. By doing so, a change in the order of the consecutive fusions corresponds to change of basis. We can define the **F-matrices**, which are essentially matrices of change of basis. For instance, given a system of three anyons a, b, c, we can write:

$$|(ab)c; ec; d\rangle = \sum_{f} (F_{abc}^{d})_{ef} \, |a(bc); af; d\rangle \, . \tag{3.35}$$

The state appearing on the left-hand side of the equation is obtained fusing a with b to obtain e, and then e with c to obtain d; on the right-hand side, the state is instead

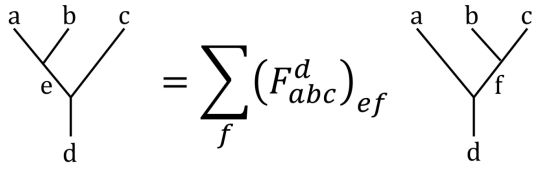

Fig. 3.5: Fusion diagrams and "change of basis", namely, change in order of the fusions. Note how the two diagrams are topologically equivalent, implying that such two diagrams corresponds to the same state of the system. Sourced from [5].

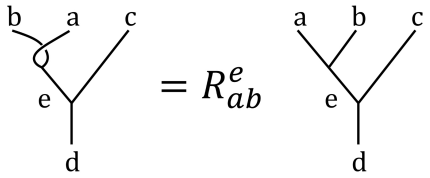

Fig. 3.6: Visual image describing the effect of applying the R-matrix. Note how, this time, the diagram on the left-hand side exhibits two ovelapping branches, which makes the two diagrams not topologically equivalent.

obtained by initially fusing b and c to obtain f, which fused with a led to d, again. Indeed, this was the process we were looking for; in a sense, it is a sort of associativity rule. In Fig.3.5, this is shown through fusion diagrams, which are very intuitive. Moreover, this notation highlights the topological nature of the problem, since the two diagrams are continuously deformed into each other, that is, they are topologically equivalent.

For everything we analyzed so far, we can understand how anyons evolve adiabatically via (3.29), i. e., through unitary operations on the fusion space that correspond to *braidings* which embody evolution at a topological level. Mathematically, these are expressed by the exchange operator we already mentioned in the previous subsection 3.2.2. From now on, we shall refer to them as **R-matrices** and denote their components with R^c_{ab}. Let us now recall the previous example, with three anyons a, b, c. Then, a clockwise exchange of a and b in the $|(ab)c; ec; d\rangle$ basis is written as:

$$|(ba)c; ec; d\rangle = \sum_f R^f_{ab}\delta_{ef}\,|(ab)c; ec; d\rangle\,. \tag{3.36}$$

The fusion diagrams version of the equation is displayed in Fig.3.6. For the presence of the Kronecker delta function δ_{ef}, a clockwise exchange is represented by a diagonal unitary matrix. The correspondent counter-clockwise exchange is represented by $R^\dagger$.

Finally, we achieve the effect of exchanging b and c clockwise in the same basis by multiplying R and F matrices:

$$|(ac)b; ec; d\rangle = (F^d_{abc})^{-1} R (F^d_{abc})\,|(ab)c; ec; d\rangle \tag{3.37}$$

where the inverse F-matrix $(F^d_{abc})^{-1}$ allows us to return to the original basis.

Ising anyons
Although this model is not able to provide a universal set for quantum computation by just braiding (we need non-topological operations to achieve it), Ising anyons are the best candidates to experiments. After addressing them, we will make use of this model in the next paragraph, "Quntum computation with anyons".

This model includes both anyons σ and fermions ψ. In this case the fusion rules are:

$$\begin{gathered} 1 \times 1 = 1, \quad 1 \times \psi = \psi, \quad 1 \times \sigma = \sigma, \\ \psi \times \psi = 1, \quad \psi \times \sigma = \sigma, \\ \sigma \times \sigma = 1 + \psi. \end{gathered} \tag{3.38}$$

The fusion space is spanned by:

$$\{|(\sigma\sigma)\sigma; 1\sigma; \sigma\rangle, |(\sigma\sigma)\sigma; \psi\sigma; \sigma\rangle\}. \tag{3.39}$$

To change basis to the one in which the first fusion involves the two left-most anyons from the right, the F-matrix takes the form:

$$F = F^{\sigma}_{\sigma\sigma\sigma} = \frac{1}{\sqrt{2}} \begin{pmatrix} 1 & 1 \\ 1 & -1 \end{pmatrix}. \tag{3.40}$$

Note the correspondence with the ordinary Hadamard gate (3.13), which maps: $|0\rangle \mapsto |+\rangle$, $|1\rangle \mapsto |-\rangle$; thus, different fusion orders imply a different basis just as the basis for a qubit can be choosen between $|0\rangle, |1\rangle$ and $|+\rangle, |-\rangle$.

We can also compute the R-matrix for the clockwise exchange of the two left-most anyons as:

$$R = \begin{pmatrix} R^1_{\sigma\sigma} & 0 \\ 0 & R^1_{\sigma\sigma} \end{pmatrix} = e^{-i\pi/8} \begin{pmatrix} 1 & 0 \\ 0 & i \end{pmatrix}. \tag{3.41}$$

It is easy to see that R^2 is a Z gate (up to an overall phase factor).

Eventually, Assume that the two rightmost items are swapped twice. The evolution of the system would have been described by:

$$F^{-1}R^2F = e^{-i4\pi} \begin{pmatrix} 0 & 1 \\ 1 & 0 \end{pmatrix}. \tag{3.42}$$

This latter expresses thus a NOT gate (apart from an overall phase factor).

As we have already mentioned at the begin of the paragraph, Ising anyons do not manage to form a universal set for quantum computing. The reason lies in the fact that they can

only implement a two-qubits gate and *Clifford gates*[12] by braiding, and together they do not form an universal set. We shall thus appeal to non-topological operations, and this of course represents a possible source of errors.

Let us instead consider a different model of non-Abelian anyons, the so-called *Fibonacci* anyons. This may be the simplest model, where the only fusion rule is: $\tau_F \times \tau_F = 1 + \tau_F$, with τ_F denoting a Fibonacci anyon. It is possible to shown that this anyons do form a universal set of quantum gates [33]. However, let us stress that the Ising model remains the best choice for experimental purposes, which is the main reason why we will be study this model instead of the Fibonacci one.

Quantum computation with anyons

We are now equipped to address a brief discussion about the real implementation of quantum computation with anyons.

To practically initialize a quantum computer, we need to create some anyons from the vacuum and fixing their position. The computational space will then be given by the fusion space of these anyons. In the case of Ising anyons (which we will consider from now on), given $2n$[13] anyons, the dimension of the fusion space will be $N = 2^{n-1}$.

Suppose we initialized the system with a certain number of anyons σ: four of them would enable one qubit, six of them can instead encode two qubits. Let us focus on the latter situation. The computational basis is:

$$\begin{aligned} |00\rangle &= |\sigma\sigma; 1\rangle \, |\sigma\sigma; 1\rangle \, |\sigma\sigma; 1\rangle \, , \\ |10\rangle &= |\sigma\sigma; \psi\rangle \, |\sigma\sigma; \psi\rangle \, |\sigma\sigma; 1\rangle \, , \\ |01\rangle &= |\sigma\sigma; 1\rangle \, |\sigma\sigma; \psi\rangle \, |\sigma\sigma; \psi\rangle \, , \\ |11\rangle &= |\sigma\sigma; \psi\rangle \, |\sigma\sigma; 1\rangle \, |\sigma\sigma; \psi\rangle \, . \end{aligned} \tag{3.43}$$

As we mentioned, to actually perform a computation in the fusion space, we need to braid anyons, i. e., we apply different sequences of R-matrices and compositions of the kind $F^{-1}RF$.

We saw above (3.40), (3.41), (3.42) how the basic single-qubit gates (correspondent to the ordinary Hadamard, Z and NOT gates) shoul appear. In the two-qubits computational

[12] Clifford gates are elements of the Clifford group, generated by the Hadamard gate, the $CNOT$ gate and the phase gate. The latter is a generalization of the Z gate, namely: $S \equiv \begin{pmatrix} 1 & 0 \\ 0 & e^{i\theta} \end{pmatrix}$, with $\theta \in \mathbb{R}$.

[13] Remember that anyons need to be created in a pairwise fashion.

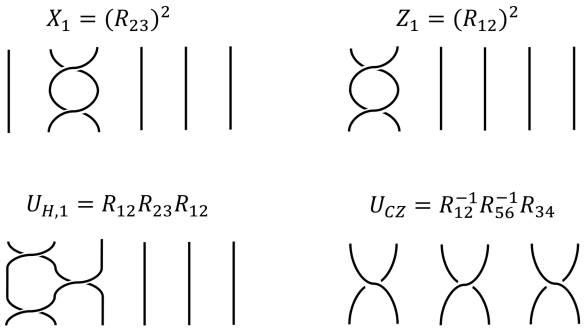

Fig. 3.7: In the figure, visual images of the braidings implementing the quantum gates discussed in the text are shown . Sourced form [5].

basis (3.43), they are expressed as:

$$\begin{aligned} U_{H,1} = R_{12}R_{23}R_{12} = RF^{-1}RFR \otimes \mathbb{I}, \quad U_{H,2} = R_{56}R_{45}R_{56} = \mathbb{I} \otimes RF^{-1}RFR, \\ X_1 = R_{23}^2 = F^{-1}R^2F \otimes \mathbb{I}, \quad Z_1 = R_{12}^2 = R^2 \otimes \mathbb{I}, \\ X_2 = R_{45}^2 = \mathbb{I} \otimes F^{-1}R^2F, \quad Z_2 = R_{56}^2 = \mathbb{I} \otimes R^2 \end{aligned} \tag{3.44}$$

where U_H coincides with the Hadamard gate up to an overall phase, the clockwise exchange operator R_{ij} acts on anyons i and j, while the subscripts on the gate symbols indicate whether they refer to the first or the second qubit.
With two qubits, we are also able to perform braiding in order to obtain a controlled-Z gate, U_{CZ}:

$$U_{CZ} = R_{12}^{-1}R_{34}R_{56}^{-1}. \tag{3.45}$$

In particular, as each R-matrix involves a different pair of anyons, it is easy to prove that $U_{CZ}\,|11\rangle = -\,|11\rangle$, which is exactly what a "conventional" CZ gate does.

Measurement process
Let us now elaborate briefly on the process of masurement.
For Ising anyons, fusion results in either the vacuum state or a ψ particle, distinguished by two different measurable changes in energy.
In a system of six anyons σ encoding two qubits, Z-basis measurements detect the fusion outcome of specific pairs (e.g., anyons 1 and 2), applying projectors like $|0\rangle\langle 0|$ or $|1\rangle\langle 1|$ based on the result. X-basis measurements similarly involve other pairs (e.g., anyons 2 and 3).

These operations project the system onto specific computational subspaces and depend on the system's microscopic details.

Possible error sources
To conclude, we shall point out that not even (real) quantum topological computers are

totally error-free. We addressed our discussion implicitly making assumptions for ideal conditions, that is zero temperature — in order to avoid any thermal excitations that could interfere with the useful anyons — and infinite separation between anyons in the degenerate subspace — so that interactions can be neglected.
Clearly, when dealing with real and practical situations, these conditions can never be fully met, inevitably resulting in some degree of decoherence.

Concerning the first assumption, studies on Abelian anyons showed that, despite the temperature being much lower that the energy gap Δ, even very small weights of thermally excited states could interfeare with anyons and the topological structure of the system. This is expected to be a problem for non-Abelian anyons, too.

Also the problem regarding infinite separation is potentially difficult to solve, as the required length scale for distance is $\xi \sim \Delta^{-1}$. Considering that, when dealing with real systems, the number of (Ising) anyons used is approximately 10^{19}, and the energy gap must be large, achieving the ideal condition becomes extremely challenging.

Moreover, in the case of Ising anyons, another source of error arises from the unavoidable need for an additional non-topological quantum gate, which will, of course, be particularly susceptible to decoherence.

To conclude, we can overall claim that, despite the challenges associated with the implementation of such technologies at the real-world level, there is considerable optimism. To grasp the potential revolutionary impact, consider that a major corporation like *Microsoft* [34] is currently dedicating substantial resources to research in this very field.

Conclusions

Through this thesis, we managed to outline a clear connection between mathematical knowledge describing geometry and processes characterizing physical systems. This approach allowed us to define many significative quantities that describe physical systems in terms of their geometric properties.

In of Chapter 2, we focused on Berry's phase (2.24), showing that its value only depends on the geometry of the closed path $\mathcal{C}$ traced by the system's Hamiltonian $\hat{H}(\mathbf{R})$ in parameter space. We then naturally introduced Berry's connection (2.26) and curvature (2.37), and found out their relations with Berry's phase. This enabled us to interpret the latter as a manifestation of holonomy associated to the local form of the connection one-form on the $U(1)$ bundle over the parameter space. Essentially, exploring this point of view through the mathematical tools addressed in Chapter 1, we ultimately proven how the concept of geometric phase is intrinsically rooted in the structure of quantum state space, emphasizing its fundamental role in quantum theory.
Furthermore, we established parallels between Berry's quantities and electromagnetic concepts. In particular, we noted how Berry's curvature is the counterpart of a magnetic field in parameters space, just as Berry's phase is the counterpart of its flux, and Berry's connection corresponds to the vector potential. These insights were applied to phenomena like the Aharonov-Bohm effect (2.60) and the behavior of systems near degeneracy points, where the curvature resembles the field of a hypothetical magnetic monopole (2.67). Extending this framework, we introduced the non-Abelian Berry's phase (2.82). The name "non-Abelian" can be traced back to the fact that the proper geometric framework to really study this concept is the one of the $U(N)$ bundle, with $N \geq 2$, a non-Abelian group. On the other hand, "ordinary" Berry's phase finds its natural framework in the $U(1)$ bundle, which is Abelian.

In Chapter 3, we explored the application of geometric and topological properties to topological quantum computation. This innovative approach stores quantum information at a topological level, making it resilient to local noise — i.e., unaffected by local geometrical details —, and thus potentially decoherence-free. This can be achieved by using an exotic type of quasiparticle, arising in two dimensions and called non-Abelian anyons. These indeed evolve through non-trivial quantum transformations governed by topology — rather than local geometry. In particular, we demonstrated that quantum states describing non-Abelian anyons would evolve via a non-Abelian Berry's phase (3.30), which is mathematically expressed by a non-trivial unitary matrix. Moving forward, our discussion delved finally into "practical" topological computation; both fusion and braiding of anyons were introduced and investigated, from either a mathematical/topological

point of view, and a conceptual one (3.33), (3.35), (3.36). Using the Ising model, we demonstrated how to construct two-qubit systems with quantum gates analogous to conventional ones. However, topological quantum computation faces significant challenges in practical implementation, including thermal excitations and the difficulty of creating and manipulating anyons.

In summary, this thesis has hopefully been able to highlight the critical role of geometry and topology in quantum processes, showing how these frameworks not only deepen our understanding, but also reveal subtle connections between different areas of physics. Such an approach often proves essential in uncovering the underlying structures governing quantum systems and their potential technological applications.

Bibliography

[1] M. V. Berry. "Quantal Phase Factors Accompanying Adiabatic Changes". In: *Proceedings of the Royal Society of London. Series A, Mathematical and Physical Sciences* 392.1802 (1984), pp. 45–57.

[2] B. M. Simon. "Holonomy, the Quantum Adiabatic Theorem, and Berry's Phase". In: *Physical Review Letters* 51.24 (1983), pp. 2167–2170. DOI: 10.1103/PhysRevLett.51.2167.

[3] F. Wilczek and A. Zee. "Appearance of Gauge Structure in Simple Dynamical Systems". In: *Physical Review Letters* 52.24 (1984), pp. 2111–2114. DOI: 10.1103/PhysRevLett.52.2111.

[4] A.Yu. Kitaev. "Fault-tolerant quantum computation by anyons". In: *Annals of Physics* 303.1 (Jan. 2003), 2–30. ISSN: 0003-4916. DOI: 10.1016/s0003-4916(02)00018-0. URL: http://dx.doi.org/10.1016/S0003-4916(02)00018-0.

[5] V.T. Lahtinen and J.K. Pachos. "A Short Introduction to Topological Quantum Computation". In: *arXiv preprint arXiv:1705.04103* (2017). Available at: https://arxiv.org/abs/1705.04103.

[6] B. F. Schutz. *Geometrical Methods of Mathematical Physics*. Cambridge, UK: Cambridge University Press, 1980.

[7] M. Nakahara. *Geometry, Topology and Physics*. 2nd. Graduate Student Series in Physics. Bristol and Philadelphia: Institute of Physics Publishing, 2003. ISBN: 9780750306065.

[8] E. W. Weisstein. *Tangent Space. MathWorld* – A Wolfram Web Resource. URL: https://mathworld.wolfram.com/TangentSpace.html.

[9] Z. Wang. *Lecture 23: Volume Forms and Orientation. University of Science and Technology of China*, Lecture Notes. p. 1. 2018. URL: http://staff.ustc.edu.cn/~wangzuoq/Courses/18F-Manifolds/Notes/Lec23.pdf.

[10] R. W. Batterman. "Falling cats, parallel parking, and polarized light". In: *Studies in History and Philosophy of Science Part B: Studies in History and Philosophy of Modern Physics* 34.4 (2003), pp. 527–557.

[11] T. Rowland. *Fiber Bundle*. https://mathworld.wolfram.com/FiberBundle.html. From MathWorld–A Wolfram Web Resource, created by Eric W. Weisstein.

[12] J. M. Lee. *Introduction to Smooth Manifolds*. 1st. New York: Springer, 2003. Chap. 8, pp. 199–200.

[13] T. Rowland. *Principal Bundle*. MathWorld–A Wolfram Web Resource, created by Eric W. Weisstein. URL: https://mathworld.wolfram.com/PrincipalBundle.html.

[14] N. Johnson. *Niles Johnson's Personal Website*. Accessed: 2024-11-18. 2024. URL: https://nilesjohnson.net.

[15] R. Mosseri and R. Dandoloff. "Geometry of entangled states, Bloch spheres and Hopf fibrations". In: *Journal of Physics A: Mathematical and General* 34.47 (2001), pp. 10243–10252.

[16] S. Pancharatnam. "Generalized Theory of Interference, and Its Applications". In: *Proceedings of the Indian Academy of Sciences - Section A* 44.5 (1956). Reprinted in Collected Works of S. Pancharatnam (Oxford University Press, UK, 1975), pp. 247–262.

[17] M. Born and V. A. Fock. "Beweis des Adiabatensatzes". In: *Zeitschrift für Physik A* 51.3–4 (1928), 165–180.

[18] J. J. Sakurai and Jim Napolitano. *Modern Quantum Mechanics*. Revised Edition. Addison-Wesley, 1994. ISBN: 978-0201539295.

[19] MIT OpenCourseWare. *L16.1 Quantum Adiabatic Theorem Stated (by B. Zwiebach)*. https://youtu.be/pgEFvhkEp-c?si=gdnYvG3$_H u29GBfS$. 2019.

[20] MIT OpenCourseWare. *L16.3 Error in the adiabatic approximation (by B. Zwiebach)*. https://youtu.be/Tcv3$_G k1Ysg?si = WxuuyVRp - hn3UqBZ$. 2019.

[21] H. Lyre. "Berry phase and quantum structure". In: *Studies in History and Philosophy of Science Part B: Studies in History and Philosophy of Modern Physics* 48 (2014), pp. 45–51. ISSN: 1355-2198. DOI: https://doi.org/10.1016/j.shpsb.2014.08.013. URL: https://www.sciencedirect.com/science/article/pii/S1355219814000975.

[22] MIT OpenCourseWare. *L17.2 Berry's phase and Berry's connection (by B. Zwiebach)*. https://youtu.be/iGG9EG3SNz0?si=EJHckYKa3EjB$_S e$. 2019.

[23] G. Morandi. *The Role of Topology in Classical and Quantum Physics*. Germany: Springer-Verlag, 1992.

[24] M. V. Berry. "The Quantum Phase, Five Years After". In: *H.H. Wills Physics Laboratory* (1988).

[25] V. I. Arnold. *Mathematical Methods of Classical Mechanics*. 1st. New York: Springer, 1978. ISBN: 978-0-387-90371-8.

[26] D. Xao, M. Chang, and Q. Niu. "Berry Phase Effects on Electronic Properties". In: *Physics Review* (2009). Oak Ridge National Laboratory, Oak Ridge, TN; National Taiwan Normal University, Taipei; The University of Texas at Austin, TX.

[27] Y. Aharonov and D. Bohm. "Significance of Electromagnetic Potentials in the Quantum Theory". In: *Physical Review* 115 (1959), pp. 485–491.

[28] M. O. Katanaev. "On geometric interpretation of the Berry phase". In: *Steklov Mathematical Institute* (2012).

[29] M. A. Nielsen and I. L. Chuang. *Quantum Computation and Quantum Information*. 10th Anniversary Edition. Cambridge, UK: Cambridge University Press, 2010. ISBN: 978-1-107-00217-3.

[30] W. H. Zurek. "Decoherence and the Transition from Quantum to Classical—Revisited". In: *Los Alamos Science* 27 (2002), pp. 2–24.

[31] W. M. Landau. *The Fundamental Group*. University of Chicago VIGRE REU Program. 2009. URL: https://www.math.uchicago.edu/~may/VIGRE/VIGRE2009/REUPapers/Landau.pdf.

[32] S. Rao. "Introduction to abelian and non-abelian anyons". In: *Lecture notes* (2017). Focus on anyon physics, fractional statistics, braid groups, and the Kitaev model.

[33] C. Nayak et al. "Non-Abelian Anyons and Topological Quantum Computation". In: *Reviews of Modern Physics* 80 (2007), pp. 1083–1159. URL: https://api.semanticscholar.org/CorpusID:119628297.

[34] E. Gibney. "Inside Microsoft's quest for a topological quantum computer". In: *Nature* (2016). URL: https://www.nature.com/articles/540523a.